Supporting Information.

Electrophilic Chemistry of Thia-PAHs: Stable Carbocations (NMR and DFT), S-Alkylated Onium Salts, Model Electrophilic Substitutions (Nitration and Bromination), and Mutagenicity Assay.

Kenneth K. Laali*, Joong-Hyun Chun, Takao Okazaki
Department of Chemistry, Kent State University, Kent, Ohio 44242

Subodh Kumar
Environmental Toxicology and Chemistry Laboratory, Great Lakes Center, State University of New York, College at Buffalo, Buffalo, New York 14222

Gabriela L. Borosky
Unidad de Matemática y Física, INFIQC, Facultad de Ciencias Químicas, Universidad Nacional de Córdoba, Ciudad Universitaria, Córdoba 5000, Argentina.

Carol Swartz
Environmental Carcinogenesis Division, US Environmental Protection Agency, Research Triangle Park, North Carolina 27711

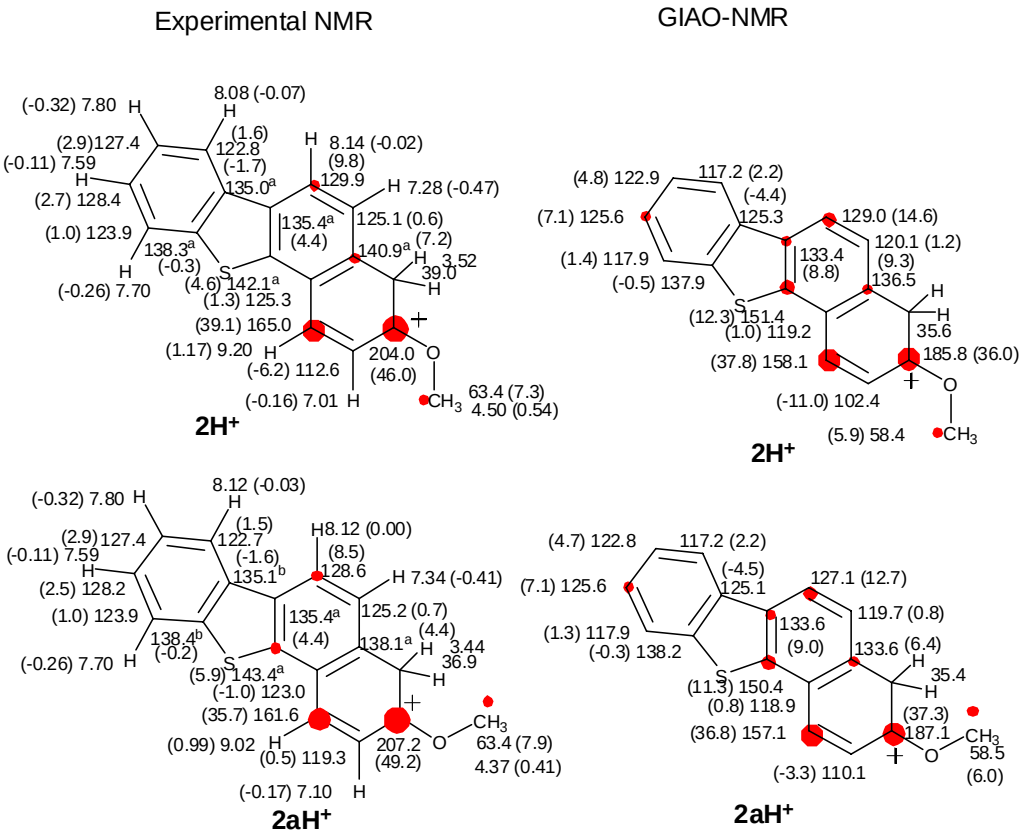

Chart S1. Experimental and GIAO/B3LYP/6-31G(d)-derived NMR chemical shifts for $\mathbf{1H}^+$, $\mathbf{1H_2}^{2+}$, $\mathbf{2H}^+$, and $\mathbf{2aH}^+$, $\Delta\delta^{13}$C values (in parentheses) relative to those for the parent PAH (red circles are roughly proportional to magnitude of $\Delta\delta^{13}$C values, threshold 5 ppm; a and b designations refer to interchangeable assignments), and changes in NPA-derived charges (Δq) for $\mathbf{1H}^+$ (dark circles are roughly proportional to C Δq, and white circle to S Δq; threshold was set to 0.030).

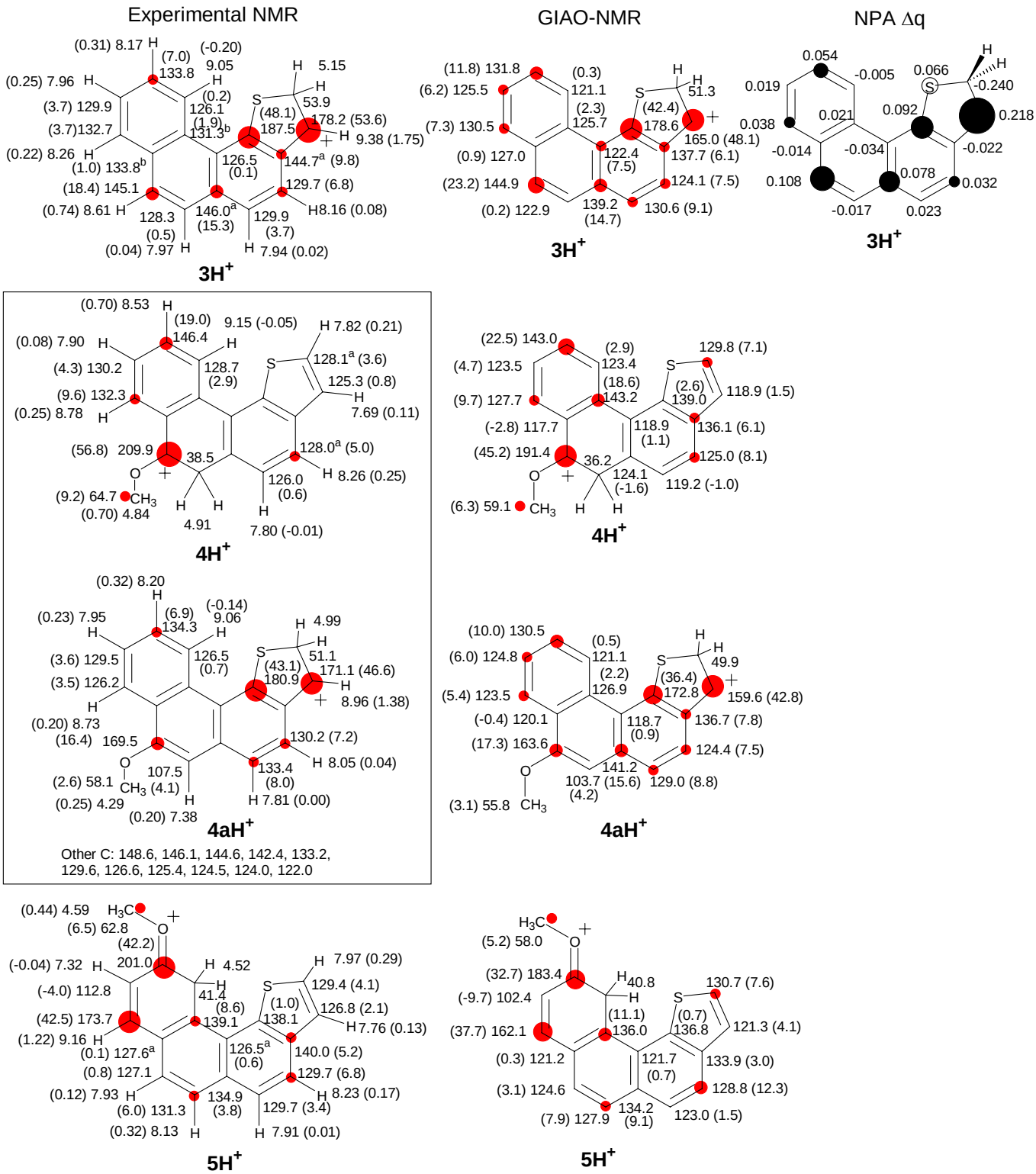

Chart S2. Experimental and GIAO/B3LYP/6-31G(d)-derived NMR chemical shifts for **3H**$^+$, **4H**$^+$, **4aH**$^+$, **5H**$^+$, **5aH**$^+$, **6H**$^+$, **6aH**$^+$, and **6bH**$^+$, $\Delta\delta^{13}$C values (in parentheses) relative to those of parent thia-PAHs (dark circles are roughly proportional to $\Delta\delta^{13}$C; threshold 5 ppm; a and b designations refer to interchangeable assignments), and changes in NPA-derived charges (Δq) for **3H**$^+$ (dark circles are roughly proportional to C Δq, and white circles to S Δq; threshold was set to 0.030).

Experimental NMR

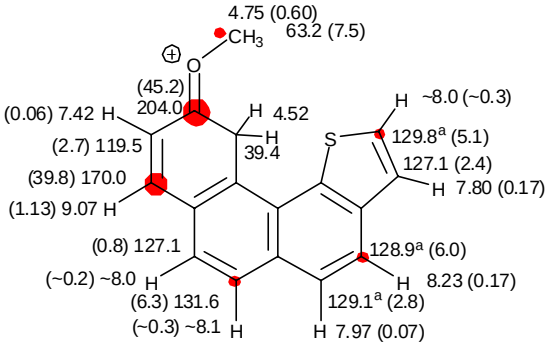

5aH⁺

GIAO-NMR

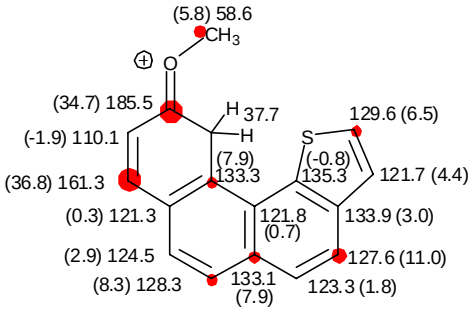

5aH⁺

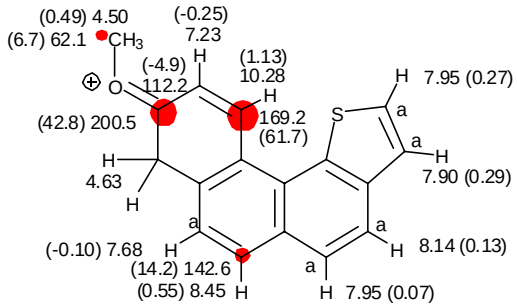

6aH⁺

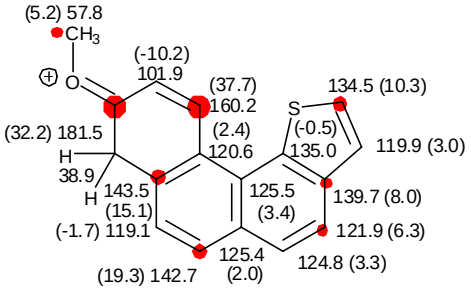

6aH⁺

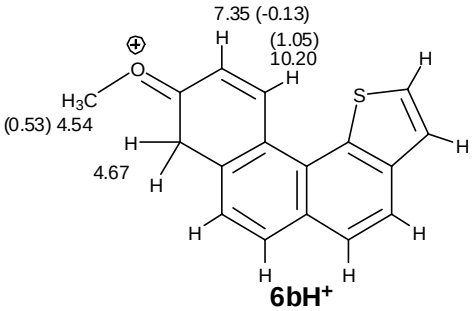

6bH⁺

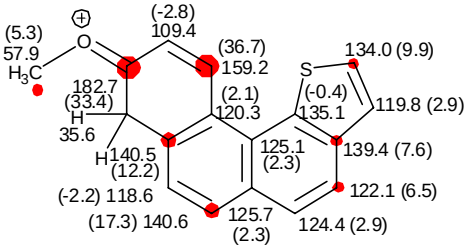

6bH⁺

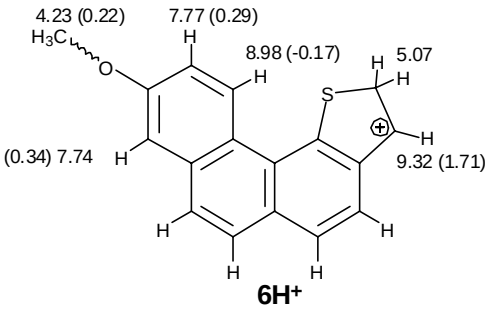

6H⁺

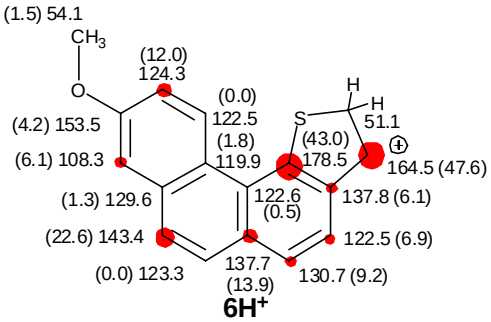

6H⁺

Chart S2 (continued).

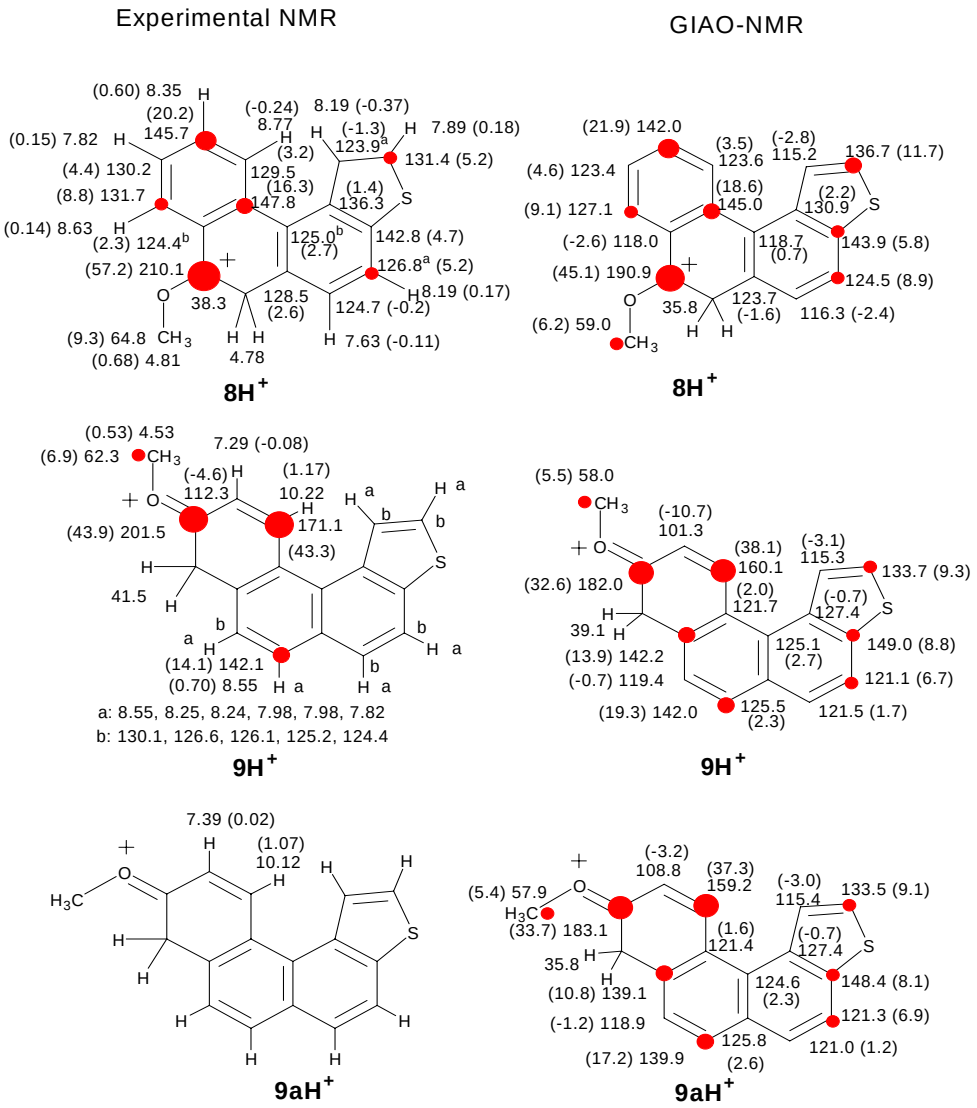

Chart S3. Experimental and GIAO/B3LYP/6-31G(d)-derived NMR chemical shifts for **7H**$^+$, **8H**$^+$, **9H**$^+$, and **9aH**$^+$, $\Delta\delta^{13}$C values (in parentheses) relative to those of parent thia-PAHs (dark circles are roughly proportional to $\Delta\delta^{13}$C values; threshold 5 ppm; a and b designations refer to interchangeable assignments, nd = not detected.

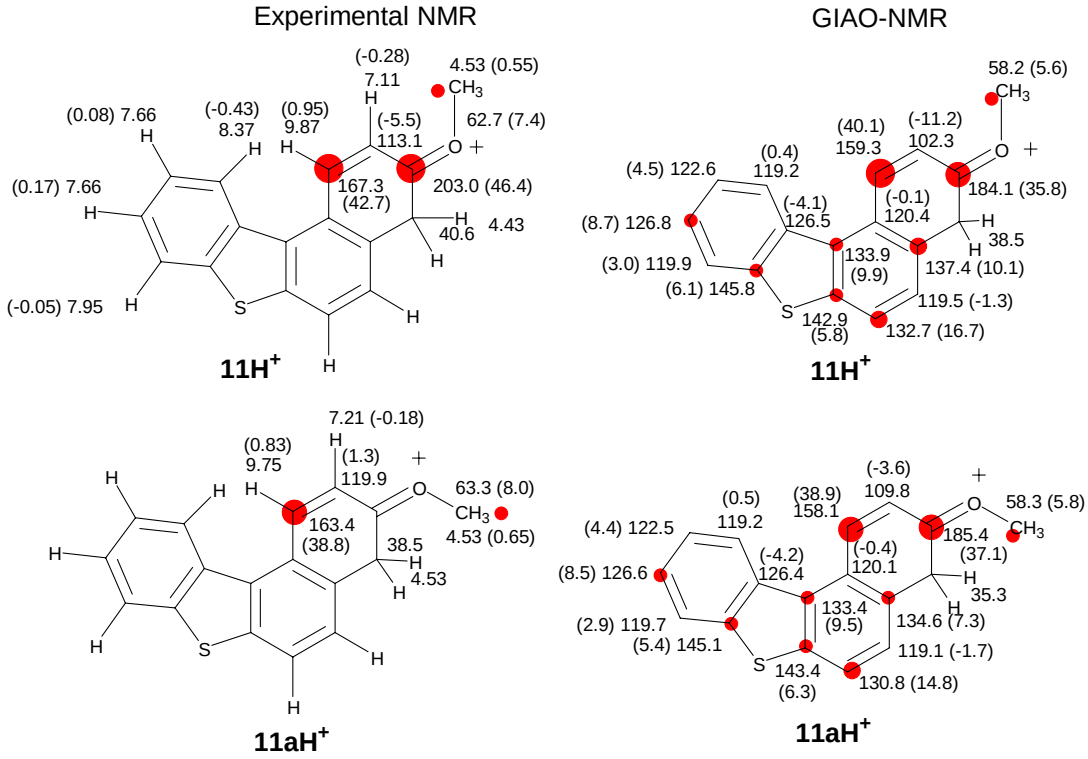

Chart S4. Experimental and GIAO/B3LYP/6-31G(d)-derived NMR chemical shifts for **11H**$^+$ and **11aH**$^+$ and $\Delta\delta^{13}$C values (in parentheses) relative to those of parent thia-PAHs (dark circles are roughly proportional to $\Delta\delta^{13}$C values; threshold 5 ppm).

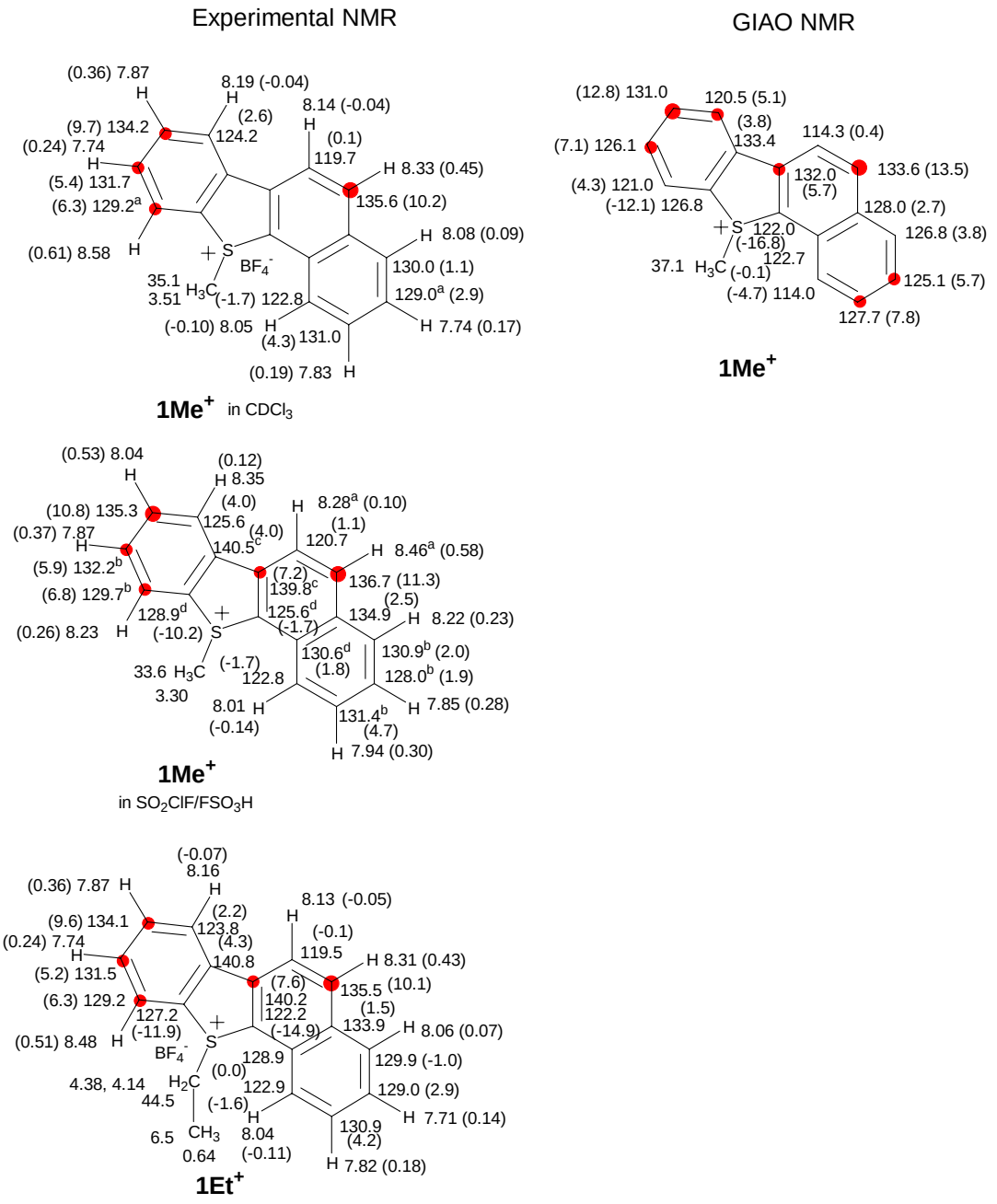

Chart S5. Experimental and GIAO/B3LYP/6-31G(d)-derived NMR chemical shifts for **1Me**$^+$, **1Et**$^+$, **10Me**$^+$, **10Et**$^+$, **12Me**$^+$, and **12Et**$^+$ and $\Delta\delta^{13}$C values (in parentheses) relative to those for the parent PAH (dark circles are roughly proportional to $\Delta\delta^{13}$C values; threshold 5 ppm; a, b, c, and d designations refer to interchangeable assignments; nd = not detected).

Experimental NMR

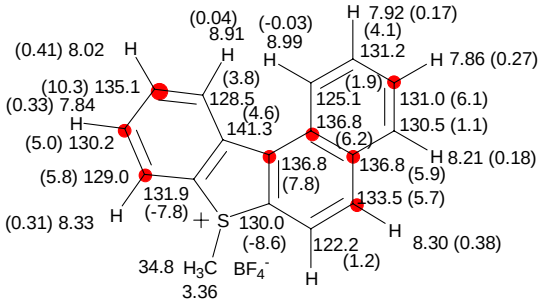

10Me$^+$

GIAO-NMR

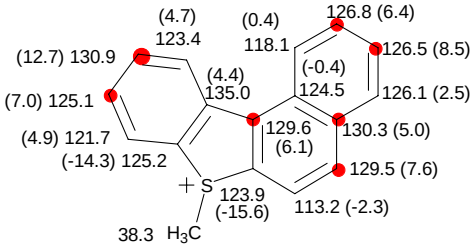

10Me$^+$

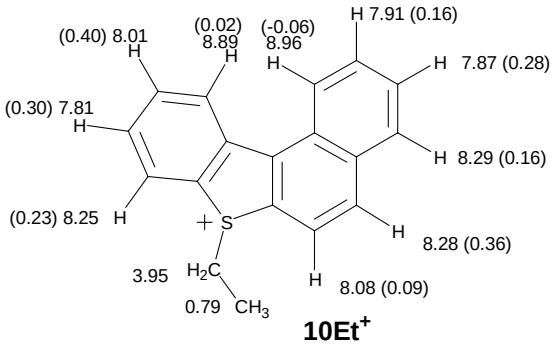

10Et$^+$

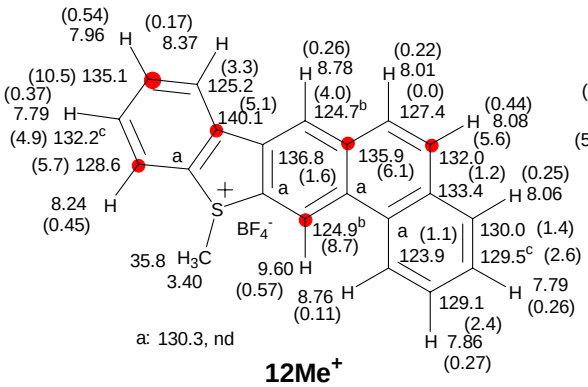

12Me$^+$

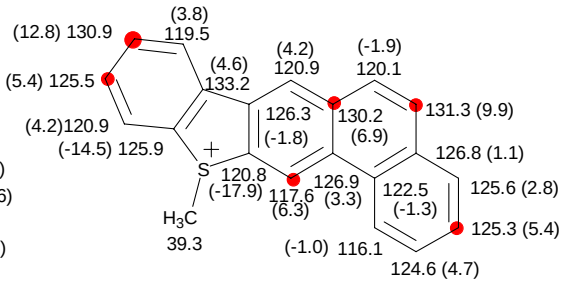

12Me$^+$

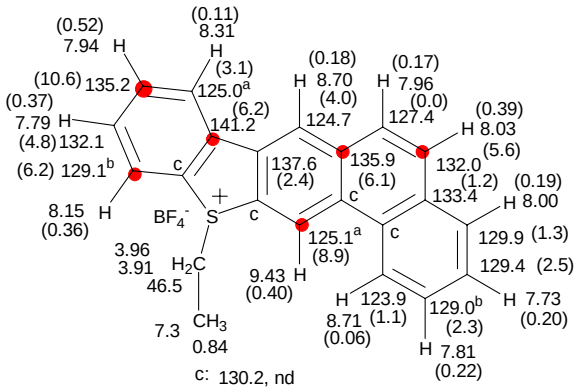

12Et$^+$

Chart S5 (continued).

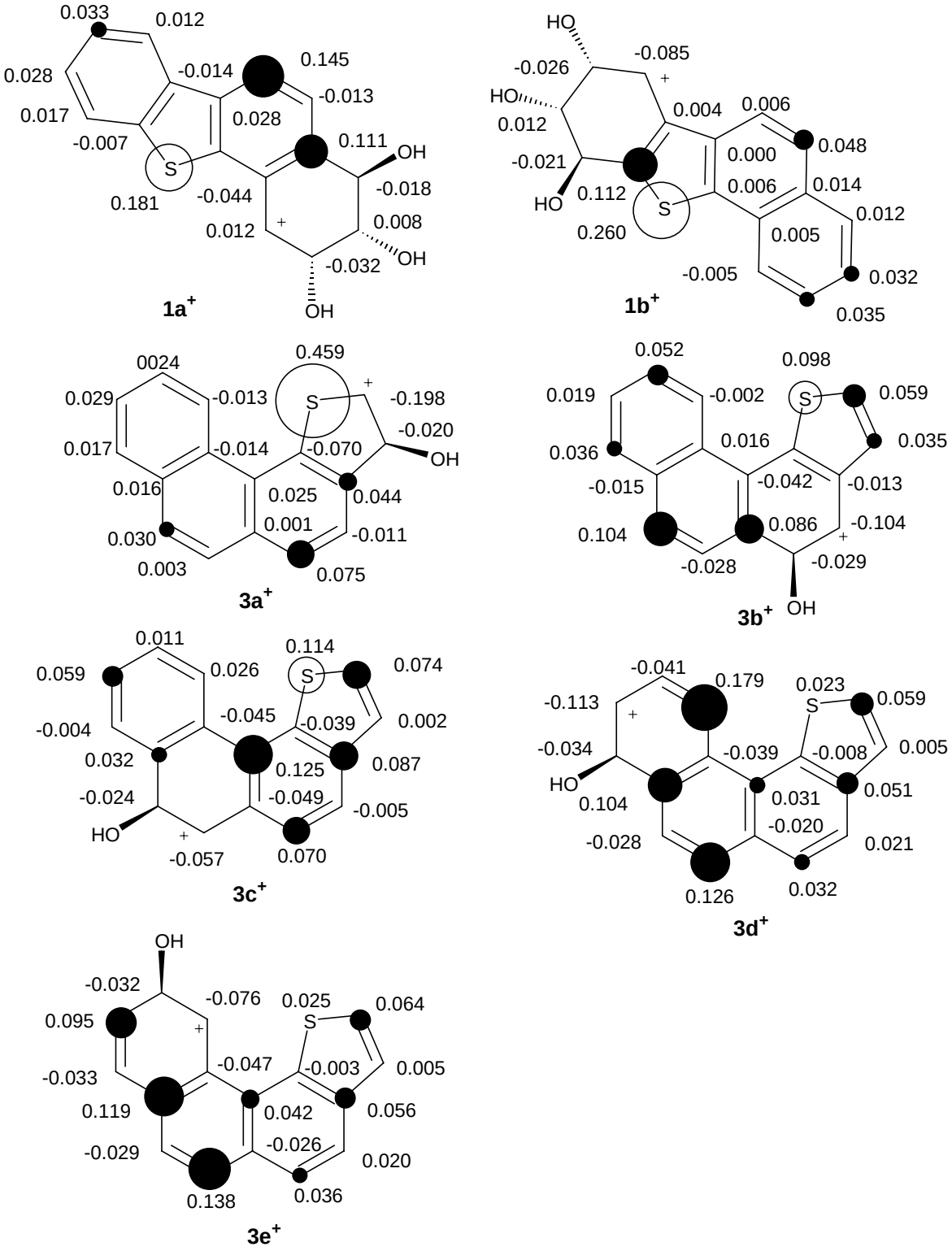

Chart S6. Changes in NPA-derived charges (Δq) for **1a**$^+$, **1b**$^+$, **3a**$^+$-**3e**$^+$, and **7a**$^+$-**7e**$^+$ relative to their corresponding epoxides (dark circles are roughly proportional to C Δq, and white circles to S Δq; threshold was set to 0.030).

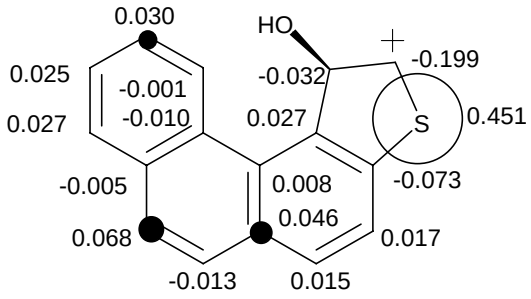

7a^{+}

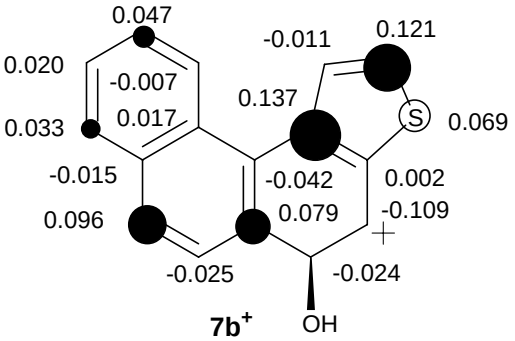

7b^{+}

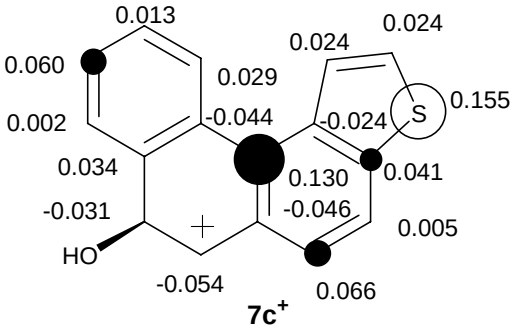

7c^{+}

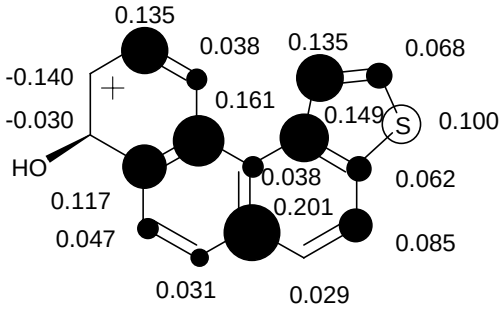

7d^{+}

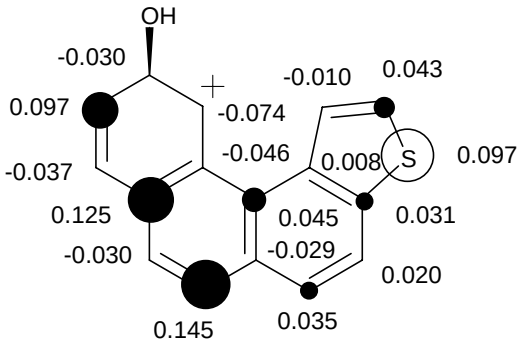

7e^{+}

Chart S6 (continued).

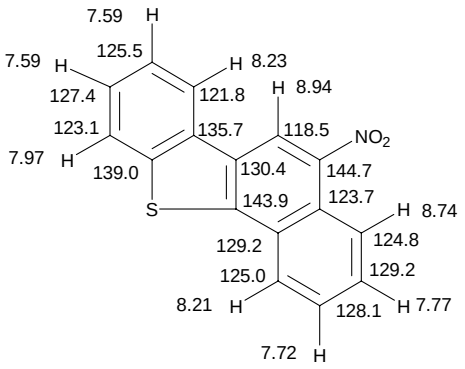

1NO$_2$

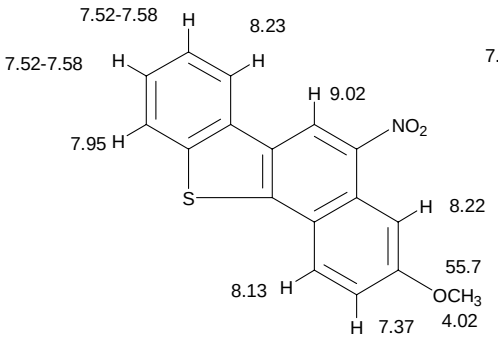

CH: 127.1, 126.7, 125.5, 123.0, 121.6, 120.4, 119.4, 103.8

2NO$_2$

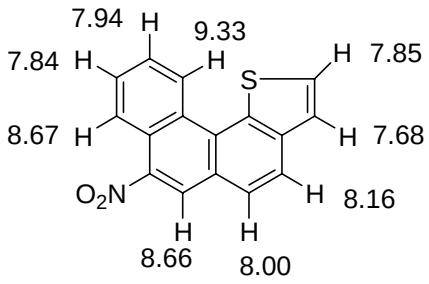

3NO$_2$

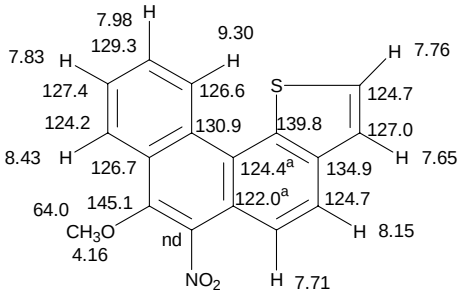

4NO$_2$

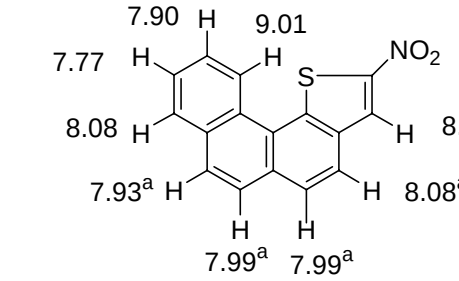

2aNO$_2$

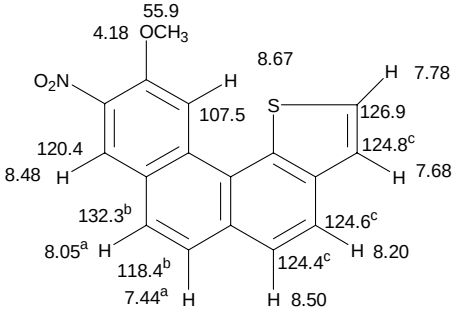

3aNO$_2$

4NO$_2$ **5NO$_2$**

Chart S7. Specific NMR assignments for the nitro- and bromo-derivatives (a, b, and c denote interchangeable assignments; nd = not detected).

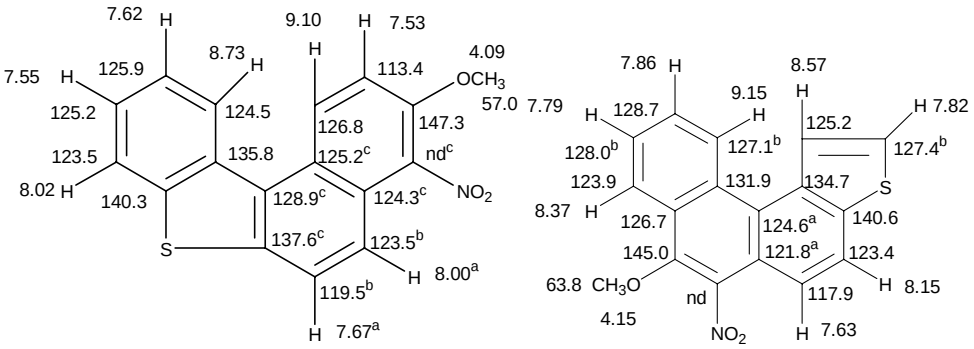

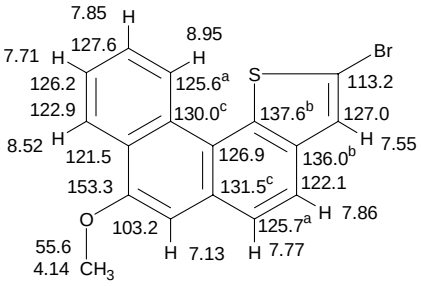

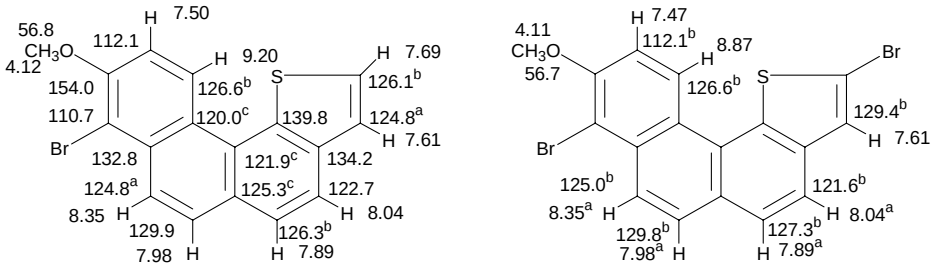

Chart S7 (continued).

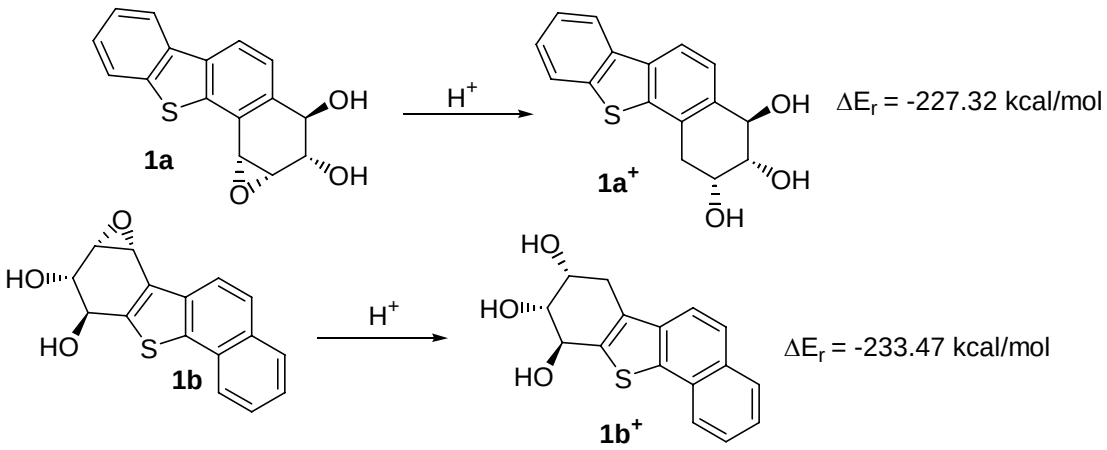

Scheme S1. Ionization reaction energies by B3LYP/6-31G(d).

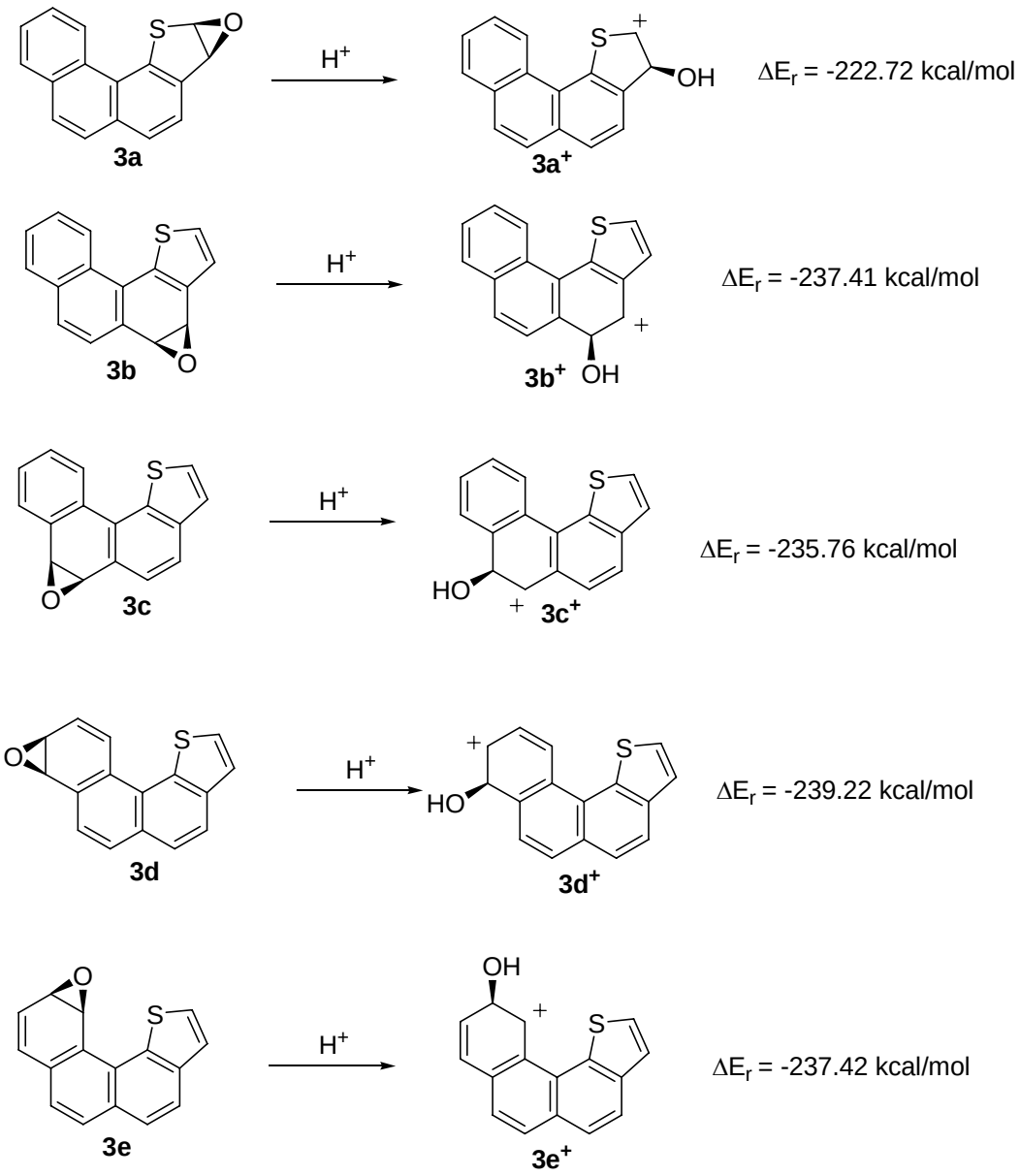

Scheme S2. Ionization reaction energies by B3LYP/6-31G(d).

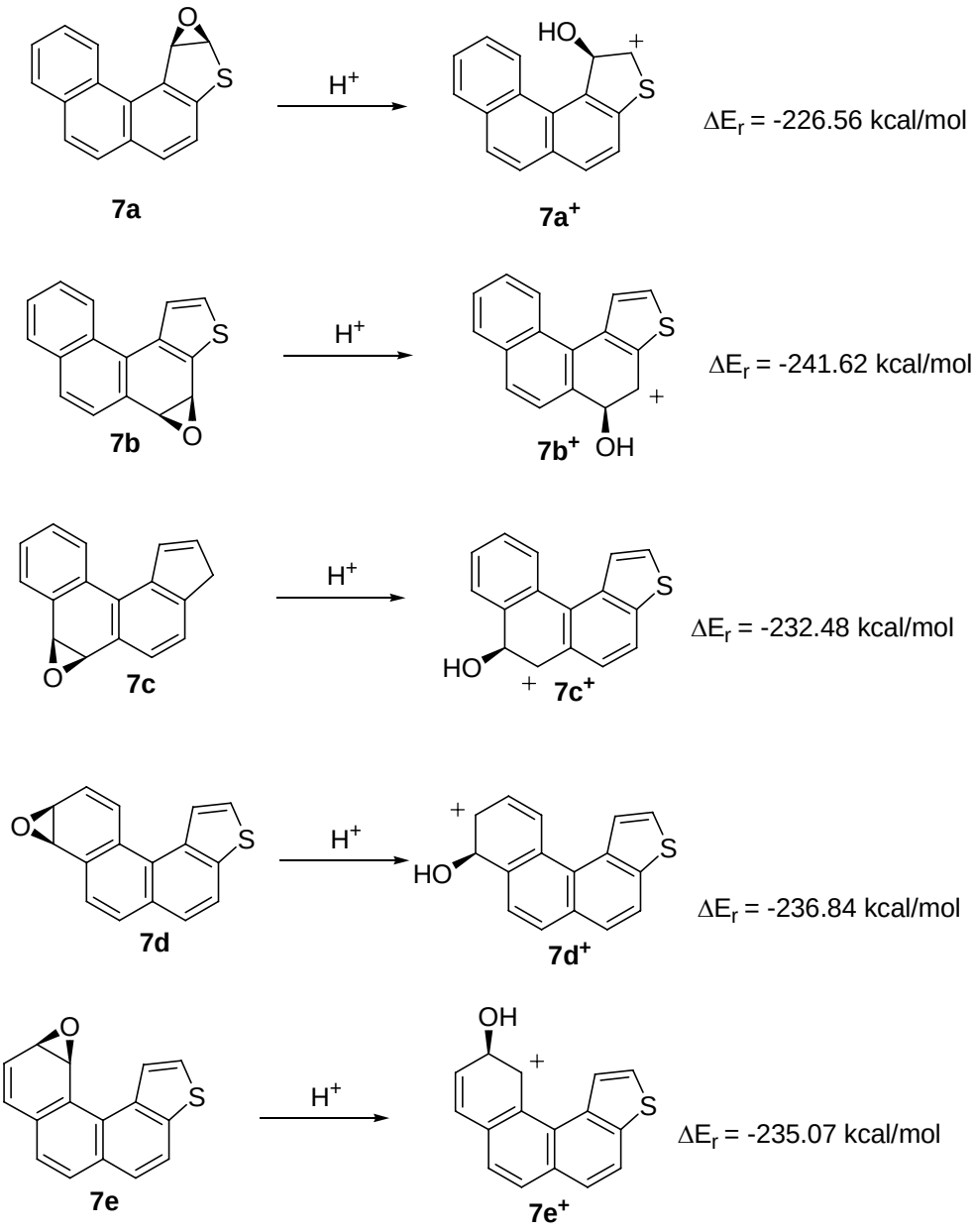

Scheme 2 (continued).

Table S1. Relative Protonation Energies for Thia-PAHs (kcal/mol) by B3LYP/6-31G(d)

Protonation site	**1**	**3**	**7**	**10**	**12**	**14**
1	4.0	28.5	10.4	1.2	8.1	2.8
2	8.8	(0.0)	(0.0)	7.1	7.6	4.8
3	6.0	14.2	28.3	5.0	8.8	7.8
4	7.2	9.2	9.5	5.8	7.5	4.6
5	(0.0)	8.1	4.4	0.0	3.4	1.4
6	7.3	11.7	9.6	7.5	7.9	6.7
7	5.4	6.5	5.9	17.9	(0.0)	(0.0)
8	7.8	10.3	8.9	9.1	10.4	4.8
9	4.1	13.0	10.4	2.7	10.1	4.8
10	10.2	10.5	9.5	6.7	8.6	8.3
11	18.1	8.2	7.3	1.6	12.6	3.4
12	-	-	-	-	19.7	10.5
13	-	-	-	-	1.6	17.9

Table S2. Energy, Zero Point Energy (ZPE), Gibbs Free Energy (G), and Relative Gibbs Free Energy (ΔG) for Optimized Structures of Thia-PAHs and their Carbocations by B3LYP/6-31G(d)

Compound	Symmetry	E, hartree	ZPE, hartree	G, hartree	ΔG,[a] kcal/mol
2	C_1	-1128.4752611	0.241236	-1128.275380	(0)
2H$^+$	C_1	-1128.8349695	0.253006	-1128.624458	-219.1
2aH$^+$	C_1	-1128.832178	0.252826	-1128.621617	-217.3
4	C_1	-1128.4627176	0.241142	-1128.263827	(0)
4H$^+$	C_1	-1128.8236828	0.252885	-1128.613088	-219.2
4aH$^+$	C_1	-1128.8317608	0.253249	-1128.620900	-224.1
5	C_1	-1128.4631576	0.240946	-1128.264168	(0)
5H$^+$	C_1	-1128.8285786	0.253131	-1128.617109	-221.5
5aH$^+$	C_1	-1128.8254823	0.252889	-1128.614332	-219.7
5bH$^+$ (9-protonation)					
	C1	-1128.8145042	0.252531	-1128.604154	-213.3
6	C_1	-1128.4631035	0.240907	-1128.264736	(0)
6H$^+$	C_1	-1128.8235637	0.252716	-1128.614082	-219.2
6aH$^+$	C_1	-1128.8250055	0.252800	-1128.614700	-219.6
6bH$^+$	C_1	-1128.8217156	0.252511	-1128.611777	-217.8
8	C_1	-1128.4594904	0.241526	-1128.259132	(0)
8H$^+$	C_1	-1128.8219681	0.253186	-1128.610703	-220.6
9	C_1	-1128.4599416	0.241323	-1128.259900	(0)
9H$^+$	C_1	-1128.8221266	0.253037	-1128.611155	-220.4
9aH$^+$	C_1	-1128.8189765	0.252807	-1128.608204	-218.6
11	C_1	-1128.468922	0.241387	-1128.269220	(0)
11H$^+$	C_1	-1128.8290267	0.253208	-1128.618171	-219.0
11aH$^+$	C_1	-1128.8262521	0.252977	-1128.615618	-217.4

[a]) Gibbs free energy relative to those of parent thia-PAH.

Table S3. Reaction Energies (kcal/mol) for Transfer-alkylation to Model Nitrogen Nucleophile Receptors by B3LYP/6-31G(d)

Sulfonium Salt	Azonium Salt				
	16Me$^+$	**17Me$^+$**	**18Me$^+$**	**18Et$^+$**	**18Pr$^+$**
1Me$^+$	-28.2	-25.9	-32.3		
3Me$^+$	-32.7	-30.5	-36.9		
3Et$^+$	-	-	-	-37.5	-
3Pr$^+$	-	-	-	-	-37.4
7Me$^+$	-33.2	-30.9	-37.4		
7Et$^+$	-	-	-	-37.8	-
7Pr$^+$	-	-	-	-	-37.7
10Me$^+$	-28.6	-26.4	-32.8		
12Me$^+$	-25.3	-23.1	-29.5		
14Me$^+$	-26.5	-24.3	-30.7		

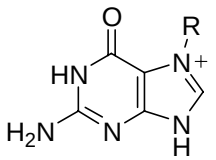

18Me$^+$ (R = Me)
18Et$^+$ (R = Et)
18Pr$^+$ (R = *n*-Pr)

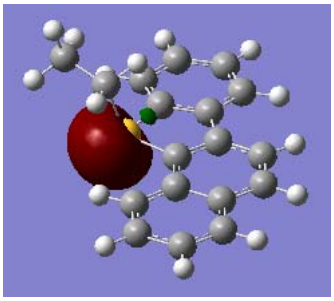

(a) lone-pair orbital at sulfur

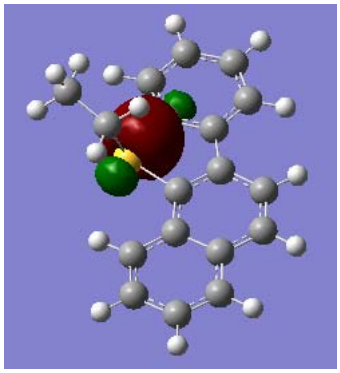

(b) bonding orbital for C-S bond

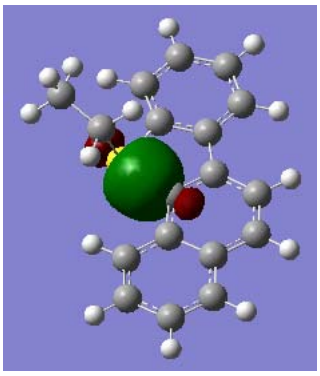

(c) bonding orbital for C-S bond

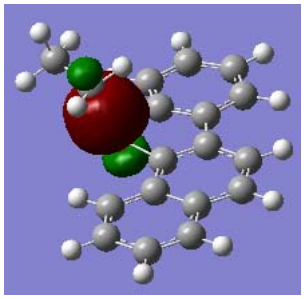

(d) bonding orbital for S-CH_2 bond

Figure S1. NBO analysis for **1Et**$^+$ by B3LYP/6-31G(d).

Experimental

General. NMR spectra were recorded at 500 MHz in low temperature stable ion studies and at 500 MHz or at 400 MHz for room temperature studies. Electrospray-MS (ES-MS) spectra for the neutral substrates and their nitro-/bromo-derivatives were obtained by infusion mode by mixing a solution of the neutral product in CH_2Cl_2 with AgOTf (30 μM) in MeOH to form PAH/Ag^+ adducts.[20] The ES-MS spectra for the onium salts were recorded by infusion mode on highly diluted acetonitrile solutions. The IR spectra were recorded on an FT-IR instrument. Synthesis of the thia-PAHs used in this study (listed in Fig 1) had already been reported by one of us (S.K.).[3,7-9,11] FSO_3H was distillated twice under argon in an all-glass distillation apparatus at atmospheric pressure and stored under argon at –20 °C in Teflon bottles with Teflon seals. SO_2ClF was prepared according to a modified procedure of Prakash et al.[21]

---

20) Laali, K. K.; Hupertz, S.; Temu, A. G.; Galembeck, S. E. *Org. Biomol. Chem.* **2005**, 3, 2319-2326.

21) Reddy, V. P.; Bellew, D. R.; Prakash, G. K. S. *J. Fluorine Chem.* **1992**, 56, 195-197.

Typical procedure for stable carbocation generation. The substrate (8-15 mg) was charged into a 5mm NMR tube, flushed with argon, and cooled to dry ice-acetone temperature. SO_2ClF (~0.4 mL) was condensed directly into the tube. Then 2-3 drops of FSO_3H were slowly added under argon to prevent local overheating, whereupon immediate color change took place. After vigorous (vortex) stirring at –78 °C, 3-4 drops of CD_2Cl_2 were slowly introduced into the NMR sample with further vigorous stirring to give a homogeneous solution.

Quenching procedure. The superacid solution was carefully poured into a cold aqueous solution of sodium bicarbonate, and extracted three times with dichloromethane. The combined organic extract was dried over magnesium sulfate, filtered, concentrated under reduced pressure, and the resulting solid residue was assayed by ^{1}H NMR. In most cases, skeletally intact substrate was recovered, along with slight degradation leading to unknown impurities (approx. 80% recovery by NMR).

Computational protocols: Structures were optimized by the density function theory (DFT) method at B3LYP/6-31G(d) level using the Gaussian 03 package.[22] All computed geometries were verified by frequency calculations to have no imaginary frequencies. E nergies of the optimized structures are summarized in Tables S1-S3 and Scheme S1 in s upporting information. NMR chemical shifts were calculated by the GIAO[23] method at the B3LYP/6-31G(d) level. NMR chemical shifts were referenced to TMS (GIAO magnetic shielding tensor = 189.8 ppm in TMS; these values are related to the GIAO isotropic magnetic susceptibility for ^{13}C), calculated with molecular symmetry of T_d at the same level of theory. Natural population analysis (NPA)-derived charges were com puted at the same level.

---

22) Frisch, M. J.; Trucks, G. W.; Schlegel, H. B.; Scuseria, G. E.; Robb, M. A.; Cheeseman, J. R.; Montgomery, J. A., Jr.; Vreven, T.; Kudin, K. N.; Burant, J. C.; Millam, J. M.; Iyengar, S. S.; Tomasi, J.; Barone, V.; Mennucci, B.; Cossi, M.; Scalmani, G.; Rega, N.; Petersson, G. A.; Nakatsuji, H.; Hada, M.; Ehara, M.; Toyota, K.; Fukuda, R.; Hasegawa, J.; Ishida, M.; Nakajima, T.; Honda, Y.; Kitao, O.; Nakai, H.; Klene, M.; Li, X.; Knox, J. E.; Hratchian, H. P.; Cross, J. B.; Adamo, C.; Jaramillo, J.; Gomperts, R.;

Stratmann, R. E.; Yazyev, O.; Austin, A. J.; Cammi, R.; Pomelli, C.; Ochterski, J. W.; Ayala, P. Y.; Morokuma, K.; Voth, G. A.; Salvador, P.; Dannenberg, J. J.; Zakrzewski, V. G.; Dapprich, S.; Daniels, A. D.; Strain, M. C.; Farkas, O.; Malick, D. K.; Rabuck, A. D.; Raghavachari, K.; Foresman, J. B.; Ortiz, J. V.; Cui, Q.; Baboul, A. G.; Clifford, S.; Cioslowski, J.; Stefanov, B. B.; Liu, G.; Liashenko, A.; Piskorz, P.; Komaromi, I.; Martin, R. L.; Fox, D. J.; Keith, T.; Al-Laham, M. A.; Peng, C. Y.; Nanayakkara, A.; Challacombe, M.; Gill, P. M. W.; Johnson, B.; Chen, W.; Wong, M. W.; Gonzalez, C.; Pople, J. A. *Gaussian 03*, Revision B.05; Gaussian, Inc.: Pittsburgh, PA, 2003.

23) Wolinski, K.; Hinton, J. F.; Pulay, P. *J. Am. Chem. Soc*. **1990**, 112, 8251-8260; Ditchfield, R. *Mol. Phys*. **1974**, 27, 789-807.

Synthesis of Onium tetrafluoroborate salts by S-alkylation:

The thia-PAH substrate (0.02 mmol) *(indicated scale was further cut down accordingly, in cases where only minuscule quantities of the thia-PAHs were available)* was dissolved in dry 1,2-dichloroethane (1 mL) at room temperature under an argon atmosphere and silver tetrafluoroborate (27.5 mg, 0.14 mmol) was added. To the resulting mixture, a solution of methyl iodide (19.8 mg, 0.14 mmol) in 1,2-dichloroethane (1 mL) was added dropwise via syringe, whereupon the reaction mixture became cloudy and a yellow solid (silver iodide) slowly precipitated out. The heterogeneous mixture was stirred at room temperature for 2 days. The resulting mixture was directly filtered off using fritted Buchner funnel (fine porous size) with a pad of celite to remove AgI. The filtered yellow solid was washed with 1, 2-dichloroethane (2 x 5 mL) and the combined filtrates were dried over $MgSO_4$, filtered, and the solvent was removed under reduced pressure. In most cases the reactions would not go to completion, and unreated substrates remained.

Numerous attempts to remove the unreacted thia-PAH from the onium salts failed due to their unexpectedly similar solubility tendencies in various solvents.

Transferalkylation to 7-azaindole – *general procedure:*

NMR scale experiments: Choice of solvent $CDCl_3$ or CD_3CN was dictated by the solubility of the onium salts. The sulfonium salt (0.01 mmol, or less depending on availability) was charged into a 5mm NMR tube and dissolved either in $CDCl_3$ or in CD_3CN (~0.6 mL). Vortex mixing gave homogeneous solutions. To the resulting solution 7-azaindole (2.8 mg, 0.02 mmol) was added, and the tube was purged with argon and vortex mixed again. The first ^1H NMR spectrum was recorded within 30 min after addition of 7-azaindole. The reaction progress was monitored by recording spectra at 30 min, 3 hrs, and 1 day intervals, during which the NMR tube was kept in the dark at r.t.

At the point when no further change in the spectra could be seen, additional 7-azaindole was added to verify reaction completion and to facilitate the interpretation of ^1H NMR spectra in aromatic region (7-azaindole peaks became larger). As summarized in Scheme 1, for **1Me**$^+$ the diagnostic methyl signal at (at δ 3.51) disappeared and and a new CH_3-singlet (δ 4.53, *N*-CH_3-) appeared within 30 min with no further changes being observed afterwards. Formation of *N*-alkylated azaindole (or imidazole) and disappearance of the initial onium salt were also verified by ES-MS.

Nitration of benzo[*b*]naphtho[2,1-*d*]thiophene 1:

General Procedure (any variations in nitric acid concentration and reaction times are indicated in Scheme 2).

Compound **1** (8.5 mg, 0.03 mmol) was dissolved in CH_2Cl_2 (2 mL). The solution was cooled to 0 ^oC (ice bath) and HNO_3 (20% *aqueous*, 2 mL) was added dropwise with

vigorous stirring. Reaction progress was monitored by TLC. After 30 min stirring at 0 ^{o}C, the reaction mixture was quenched with 30% $NaHCO_3$ (10 mL). The biphasic mixture was allowed to separate and the organic layer was extracted with CH_2Cl_2 (3 × 5 mL). The combined organic extracts were dried over $MgSO_4$, filtered, and the solvent was removed under reduced pressure. After purification of crude material to remove minor impurities by preparative TLC with CH_2Cl_2/hexane (2:8) as eluent, **1NO$_2$** was obtained as a bright yellow solid. yield, 6.4 mg (76 % isolate yield).

Bromination of 7-Methoxyphenanthro[4,3-*b*]thiophene 4:

Typical procedure- To a solution of thia-PAH **4** (6.4 mg, 0.02 mmol) in acetonitrile (5 mL) *N*-bromosuccinimide (5.3 mg, 0.03 mmol) was added at once with vigorous stirring. The reaction mixture was heated under reflux for 8 hours and the reaction progress was monitored by TLC. After 8 hrs reflux, the reaction mixture was washed with brine (10 mL) and extracted with CH_2Cl_2 (3 × 5 mL). The combined organic extracts were dried over $MgSO_4$, filtered, and the CH_2Cl_2 was removed under reduced pressure. After purification of the crude material to remove unreacted **4** and impurities by preparative TLC with CH_2Cl_2/hexane (4:6) as eluent, **4Br** was obtained a beige solid; yield, 4.6 mg (56%).

Mutagenicity Assays by Ames Test:

Thia-PAHs **1**, **5**, and **11** and their nitro derivatives **1NO$_2$**, **5NO$_2$**, and **11NO$_2$** were tested for mutagenicity toward Salmonella typhimurium strain TA100 (from Dr. Bruce Ames, University of California, Berkley). Benzo[*a*]pyrene (BaP), 1-nitropyrene (1-NP), sodium azide (NaN_3), and 2-anthramine (2A) were used as positive controls.

Plate Incorporation Assays: Aliquots were made into 2 mg/mL stock solutions in DMSO. Compounds **1** and **1NO$_2$** were tested at doses used in previously published studies,[4,5](given in Table S4 below). Compounds **5** and **11** were tested at an initial dose range of 2-80 μg/plate in the presence of S9 mix (with metabolic activation) only. Their nitro derivatives were initially tested over a dose range of 0.25-20 ug/plate (given in Table 2 below), both with and without S9 mix. Doses were adjusted in later assay replicates to better define the linear dose range for each compound. Nitro-substituted compounds were tested without S9 due to the fact that many nitro-PAHs are direct acting mutagens in the *Salmonella* assay. A standard plate incorporation method was used; the assay mix contained the test compound at various doses, 500 μl of S9 mix when used, and 100 μl of an overnight culture of *Salmonella* TA100. The plates were incubated for 3 days at 37 °C and counted on an automated colony counter. Potencies are reported as revertants/nmol (Table 1), so that activities could be compared among the compounds. BaP and 2A were used as a positive control for assays with metabolic activation and 1-NP and NaN_3 were used as controls for assays without S9 mix.

Table S4. Linear dose range with and without S9 mix.

Compound	With S9 mix	Without S9 mix
1	0-40	---
5	0-5	---
11	Not active- no linear dose range	---
1NO$_2$	0-3	0-1
5NO$_2$	0-5	0-0.25
11NO$_2$	0-20	Not active-no linear dose range

The potencies of **1** and **1NO$_2$** agree with previously published results,[4,5] except that here, **1NO$_2$** has similar potencies both with and without metabolic activation (this

compound was previously reported to induce more revertants with metabolic activation[5]). Compound **11** was inactive in the assay (tested only with metabolic activation). **11NO$_2$** was inactive without metabolic activation and only weakly mutagenic with metabolic activation. Whereas compound **5** was moderately active with metabolic activation, its nitro derivative, **5NO$_2$** was approximately twice as potent as the parent compound with metabolic activation. However, without metabolic activation, **5NO$_2$** was found to act as an extremely powerful direct-acting mutagen. Metabolism by enzymes in the S9 mix appears to inactive this compound.

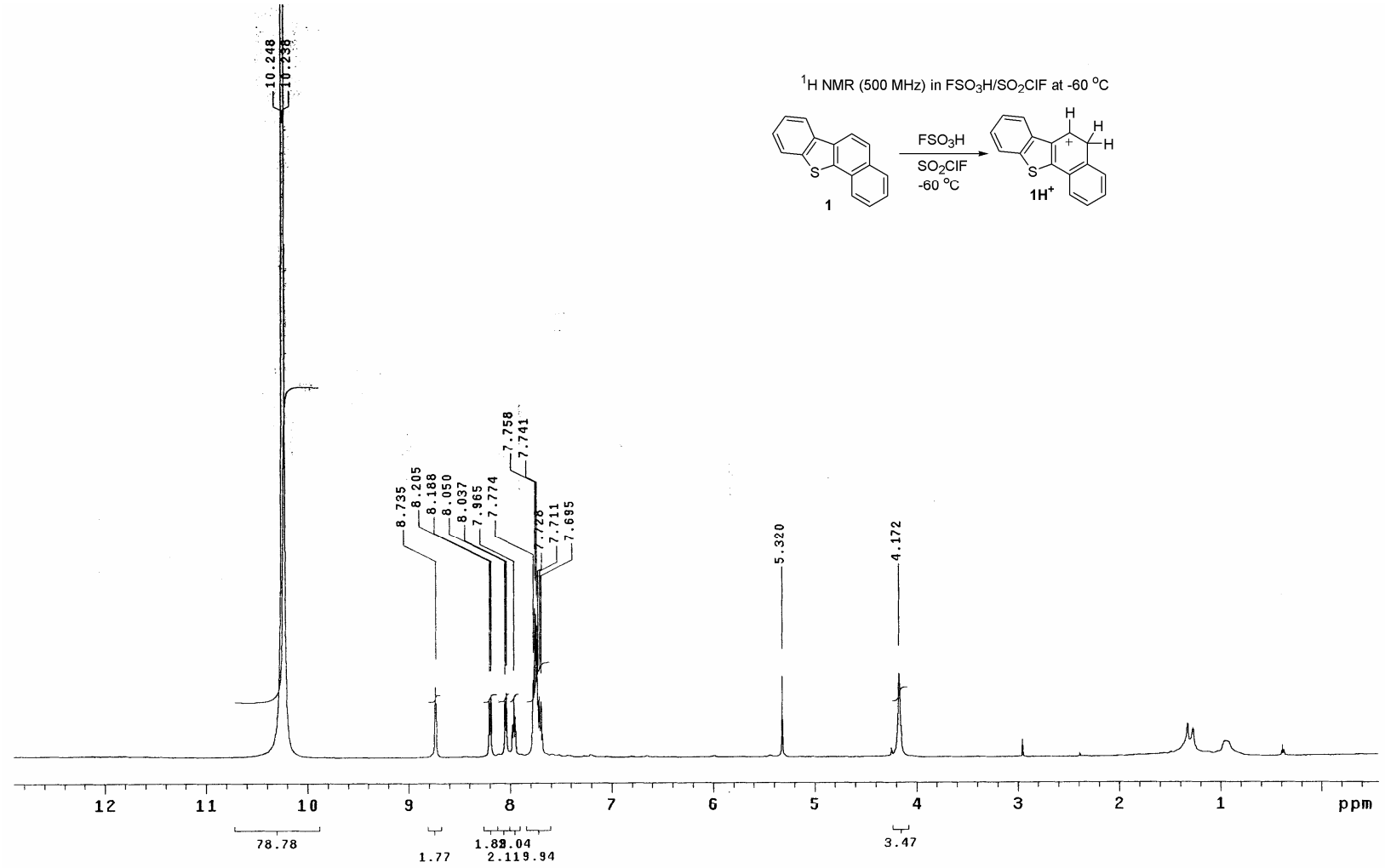

Figure S2. ^{1}H NMR spectrum of **1H**$^+$ in FSO_3H/SO_2ClF at -60 °C

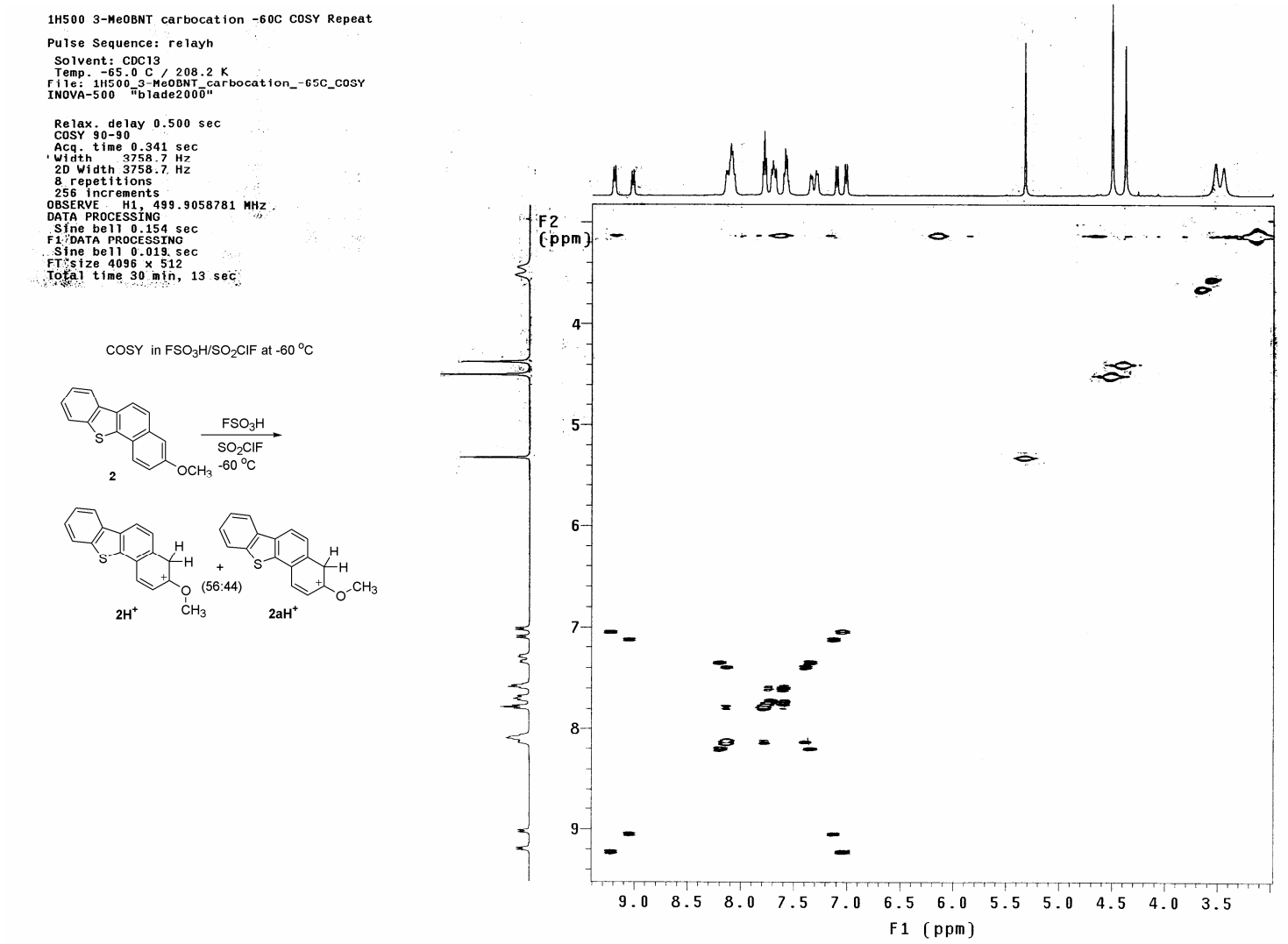

Figure S3. H/H COSY spectrum of **2H$^+$/2aH$^+$** in FSO_3H/SO_2ClF at -60 °C.

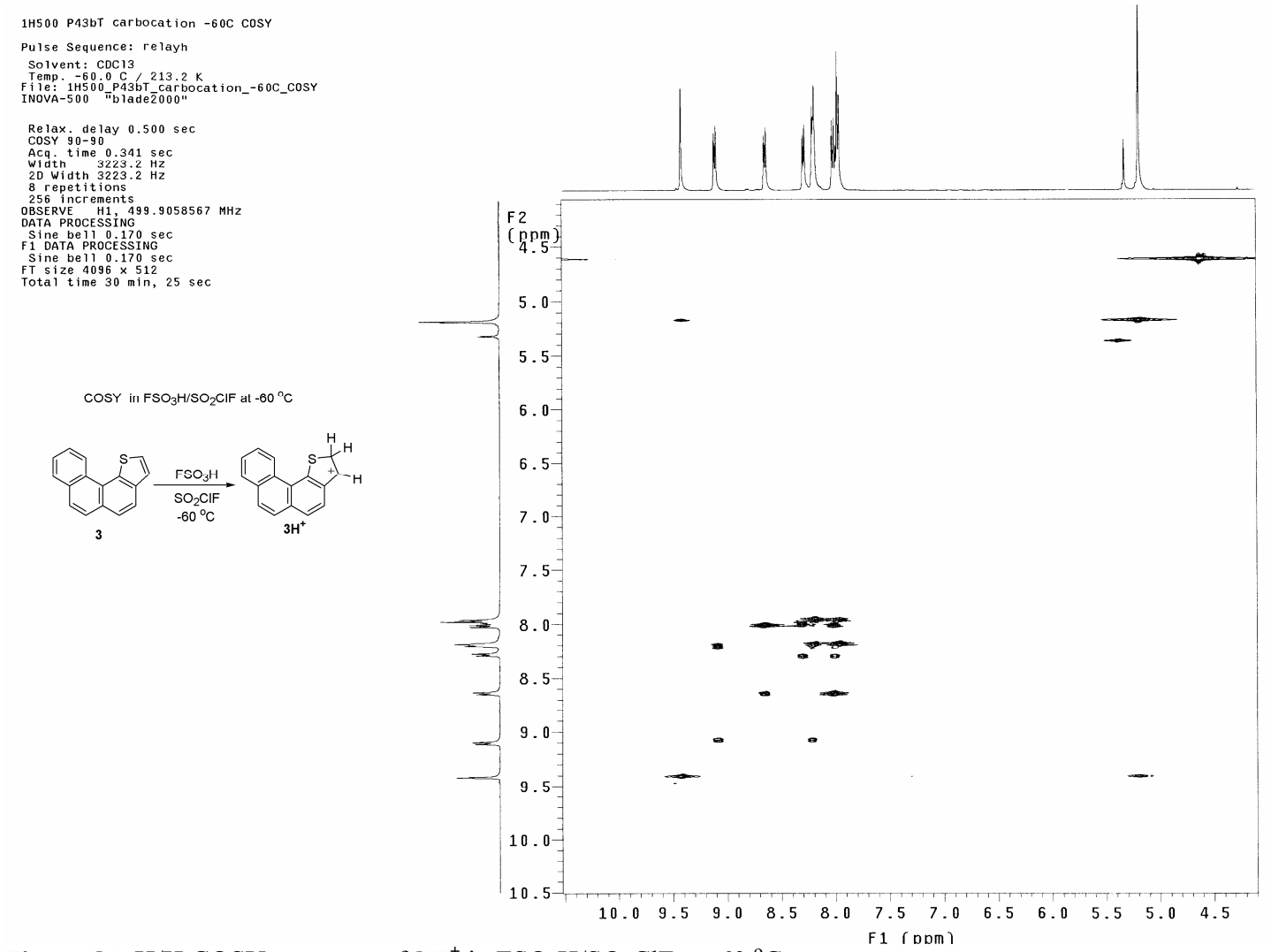

Figure S4. H/H COSY spectrum of **3H**$^+$ in FSO_3H/SO_2ClF at -60 ^oC.

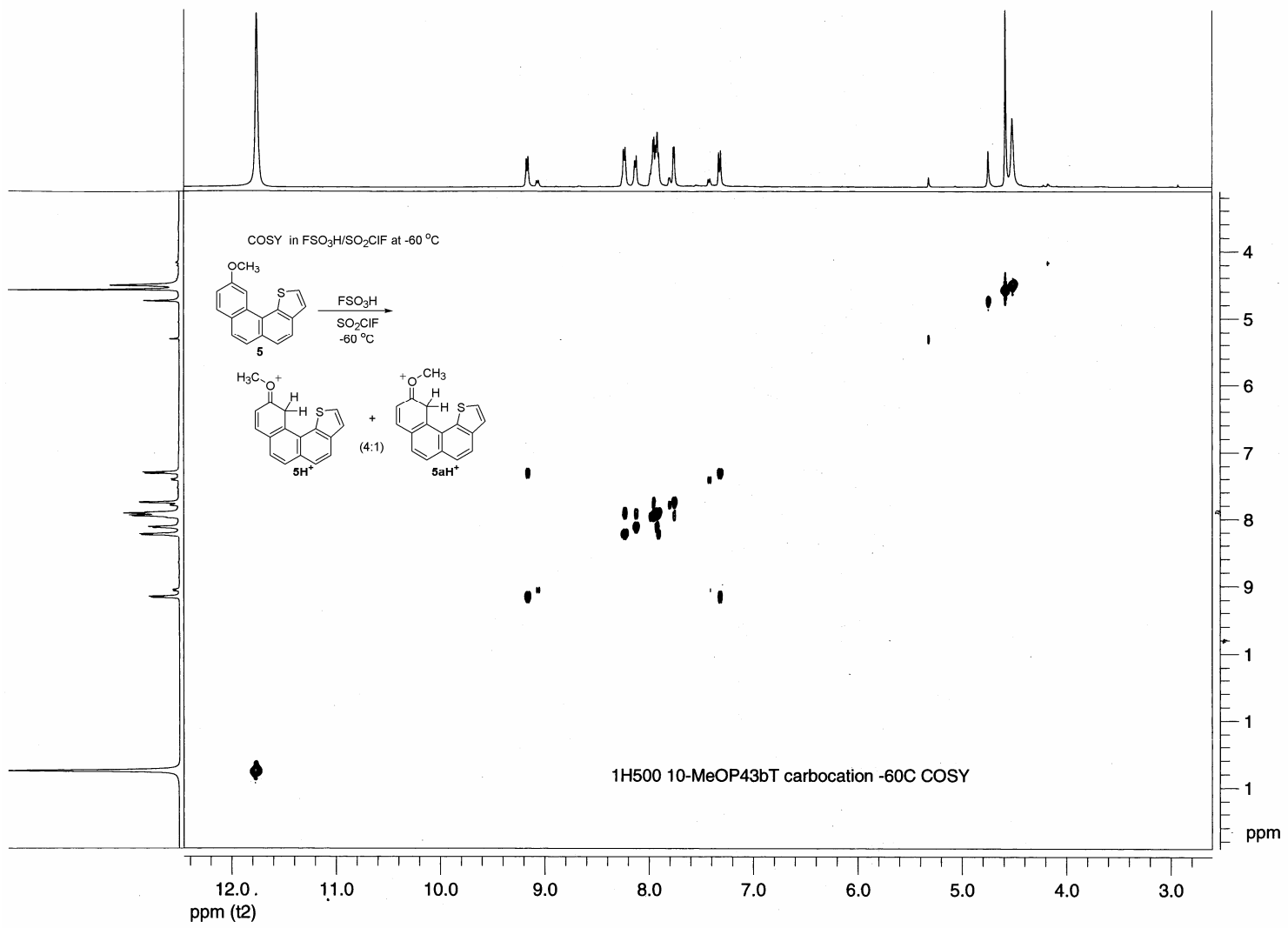

Figure S5. H/H COSY spectrum of **5H**$^+$/**5aH**$^+$ in FSO_3H/SO_2ClF at -60 ^oC

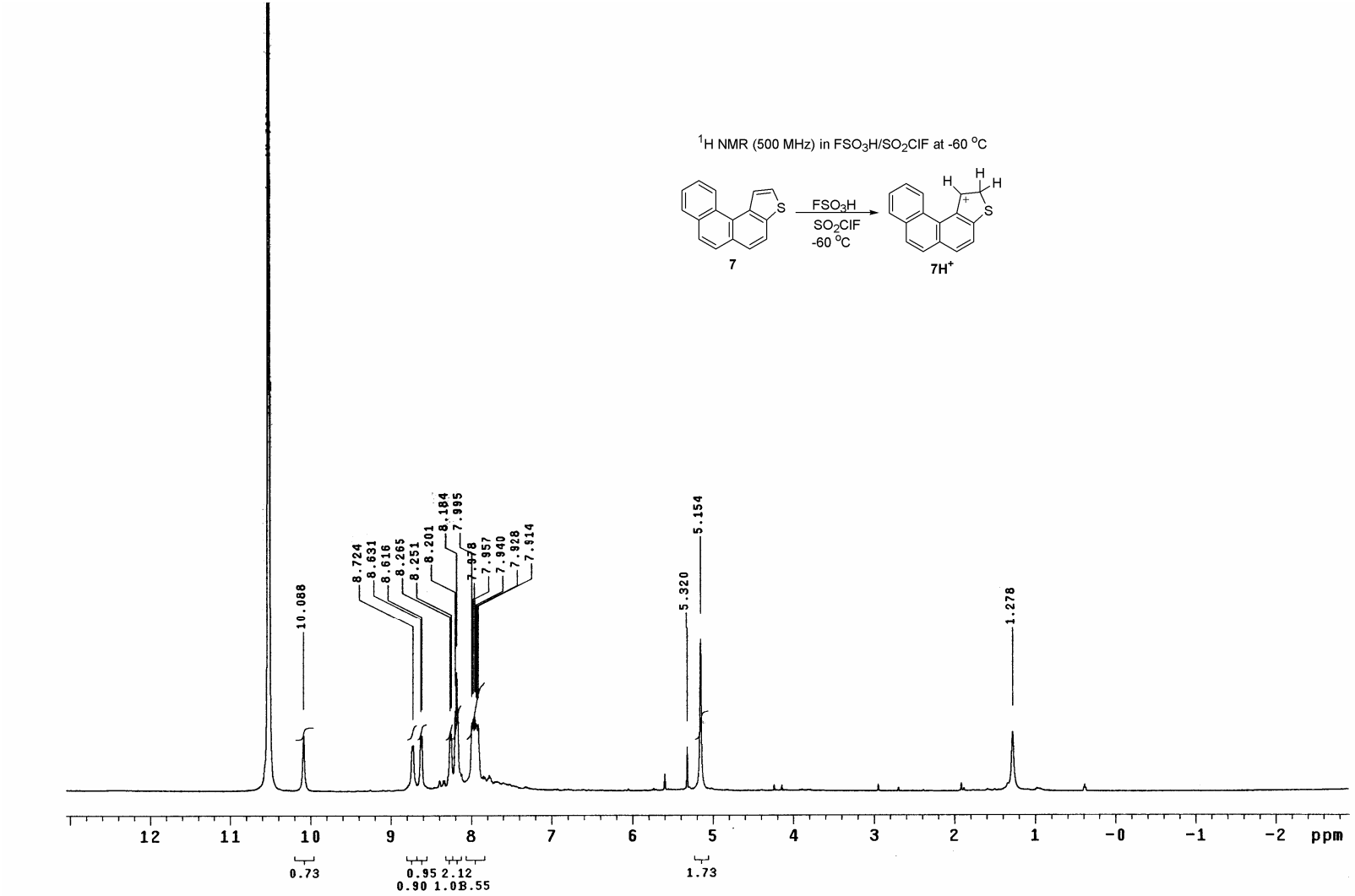

Figure S6. ^{1}H NMR spectrum of **7H**$^+$ in FSO_3H/SO_2ClF at -60 °C

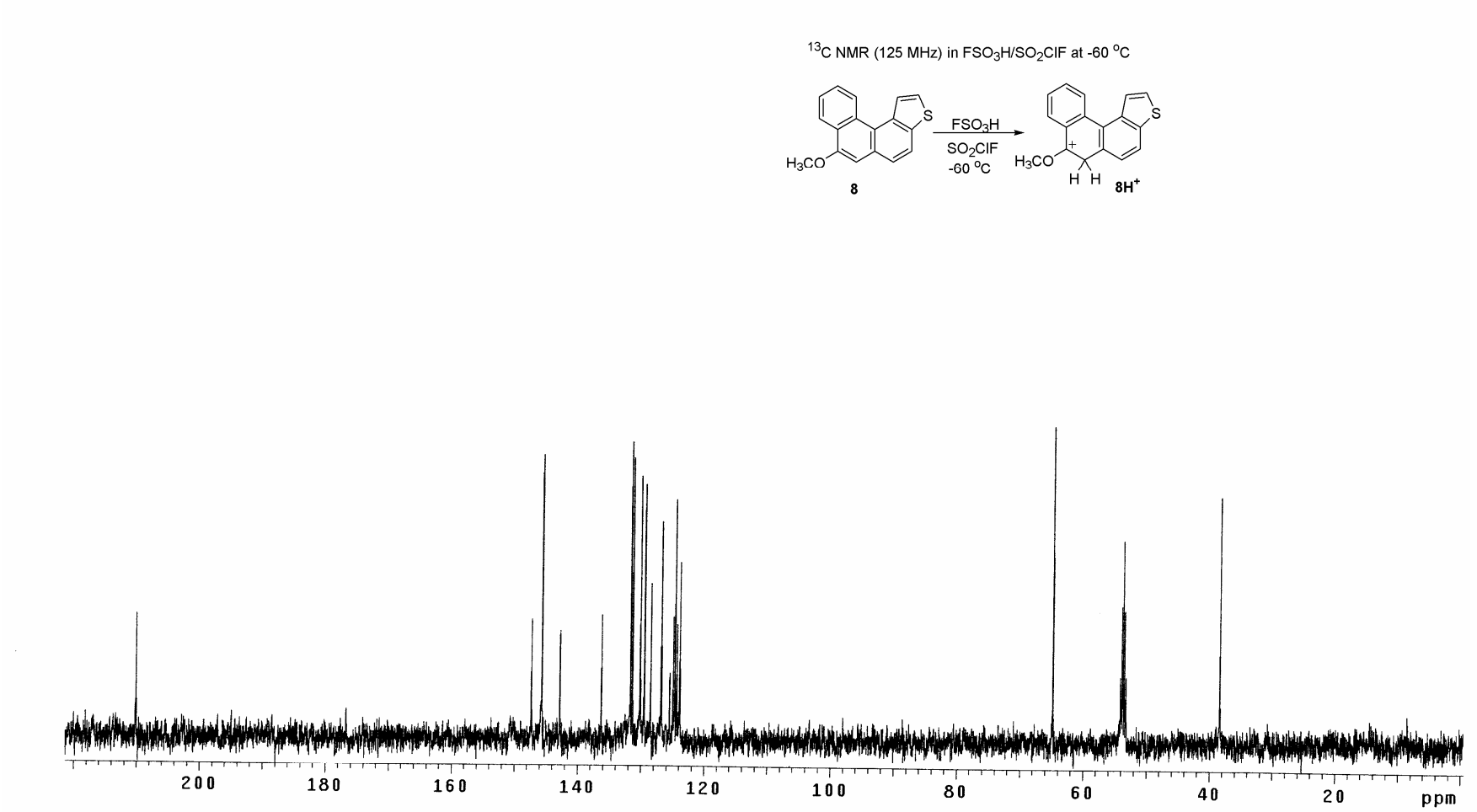

Figure S7. ^{13}C NMR spectrum of **8H**$^+$ in FSO_3H/SO_2ClF at -60 °C

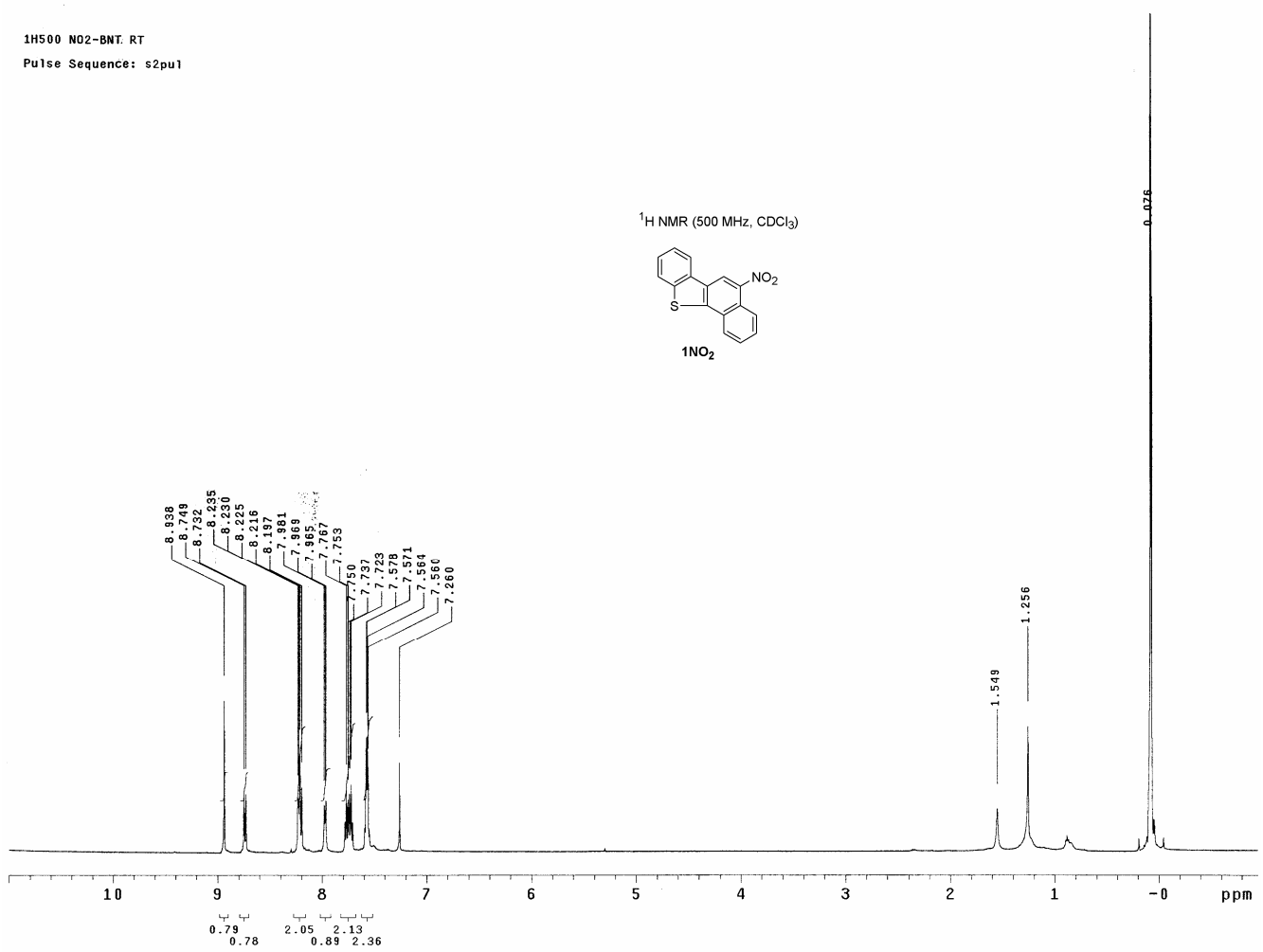

Figure S8. ^{1}H NMR spectrum of **1NO$_2$**.

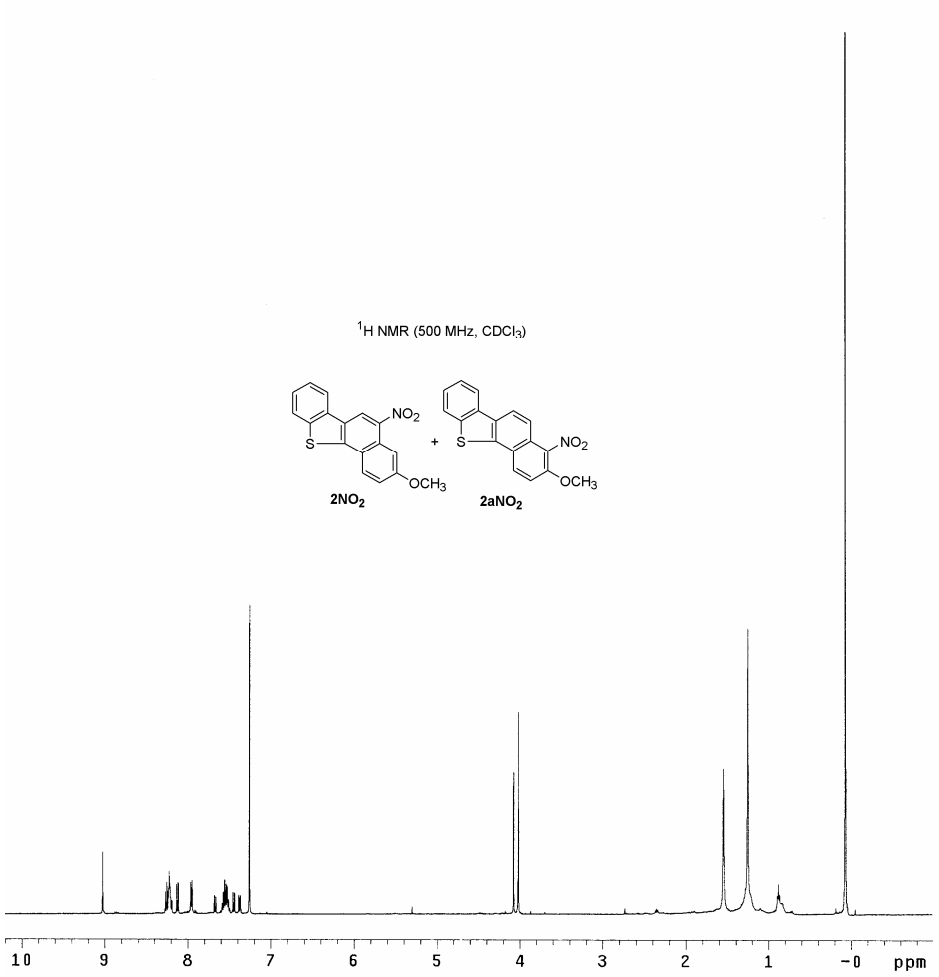

Figure S9. ^{1}H NMR spectrum of isomeric mixture of **2NO$_2$** and **2aNO$_2$**.

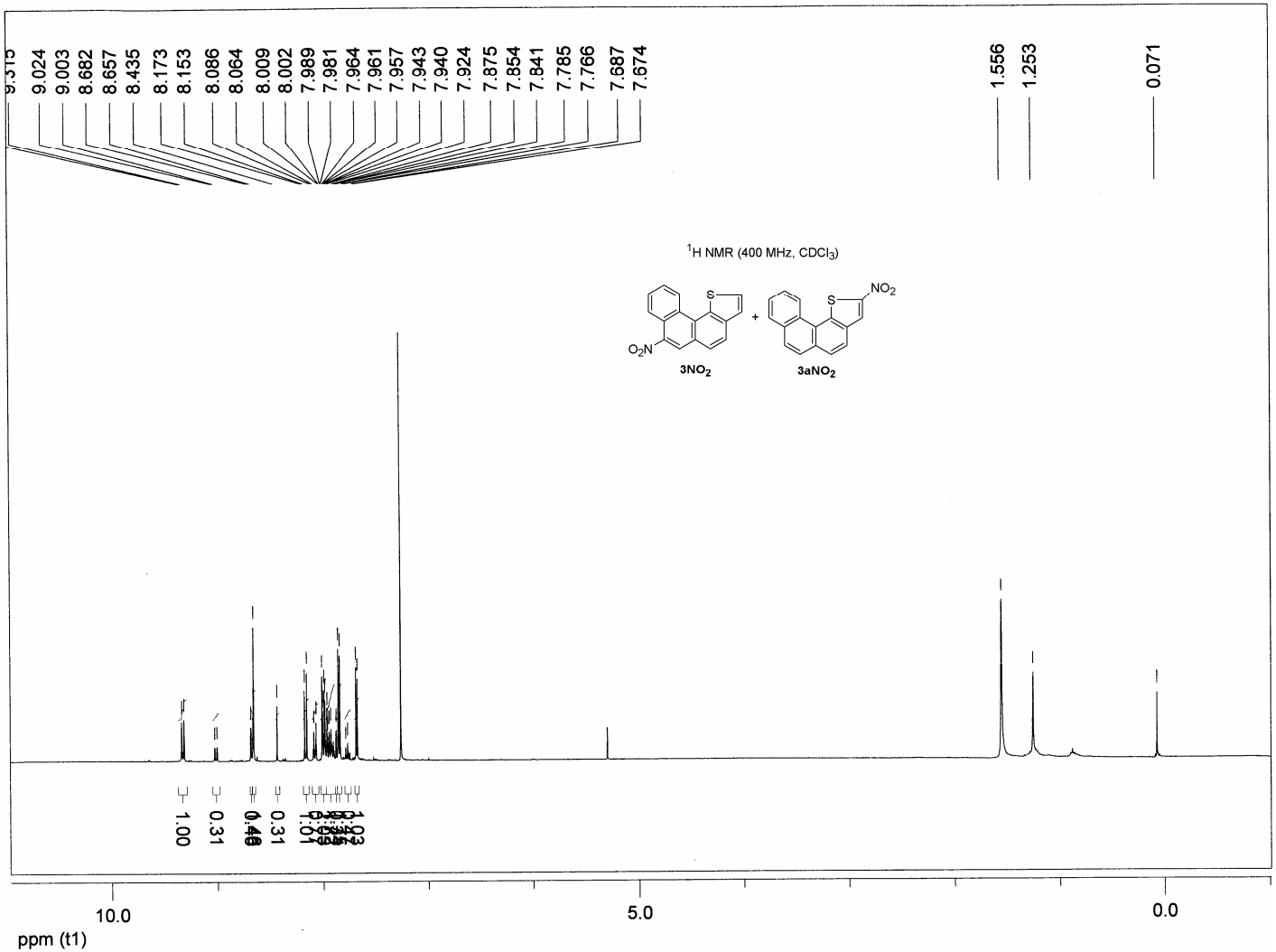

Figure S10. ^{1}H NMR spectrum of isomeric mixture of **3NO$_2$** and **3aNO$_2$**.

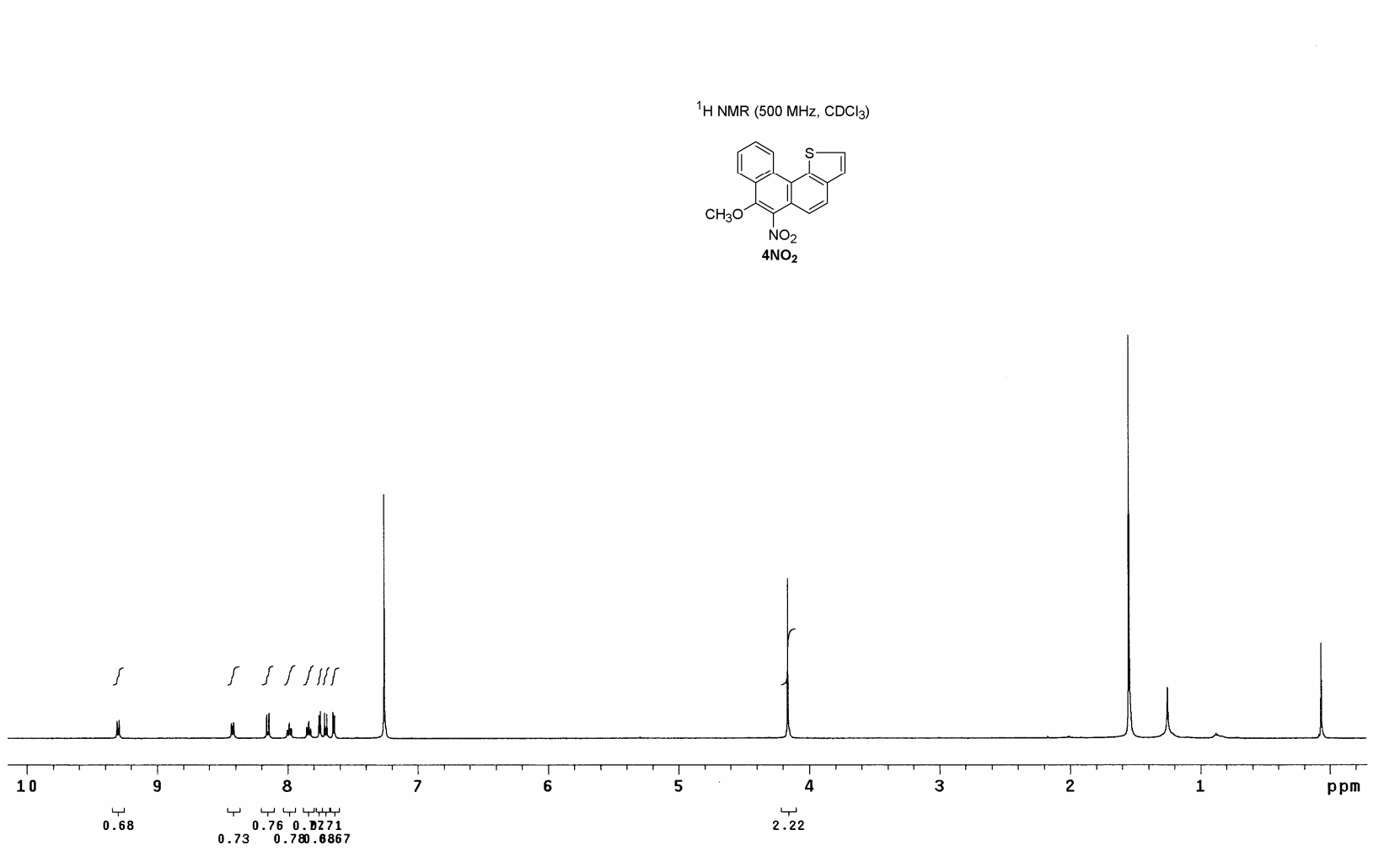

Figure S11. ^{1}H NMR spectrum of **4NO_2**.

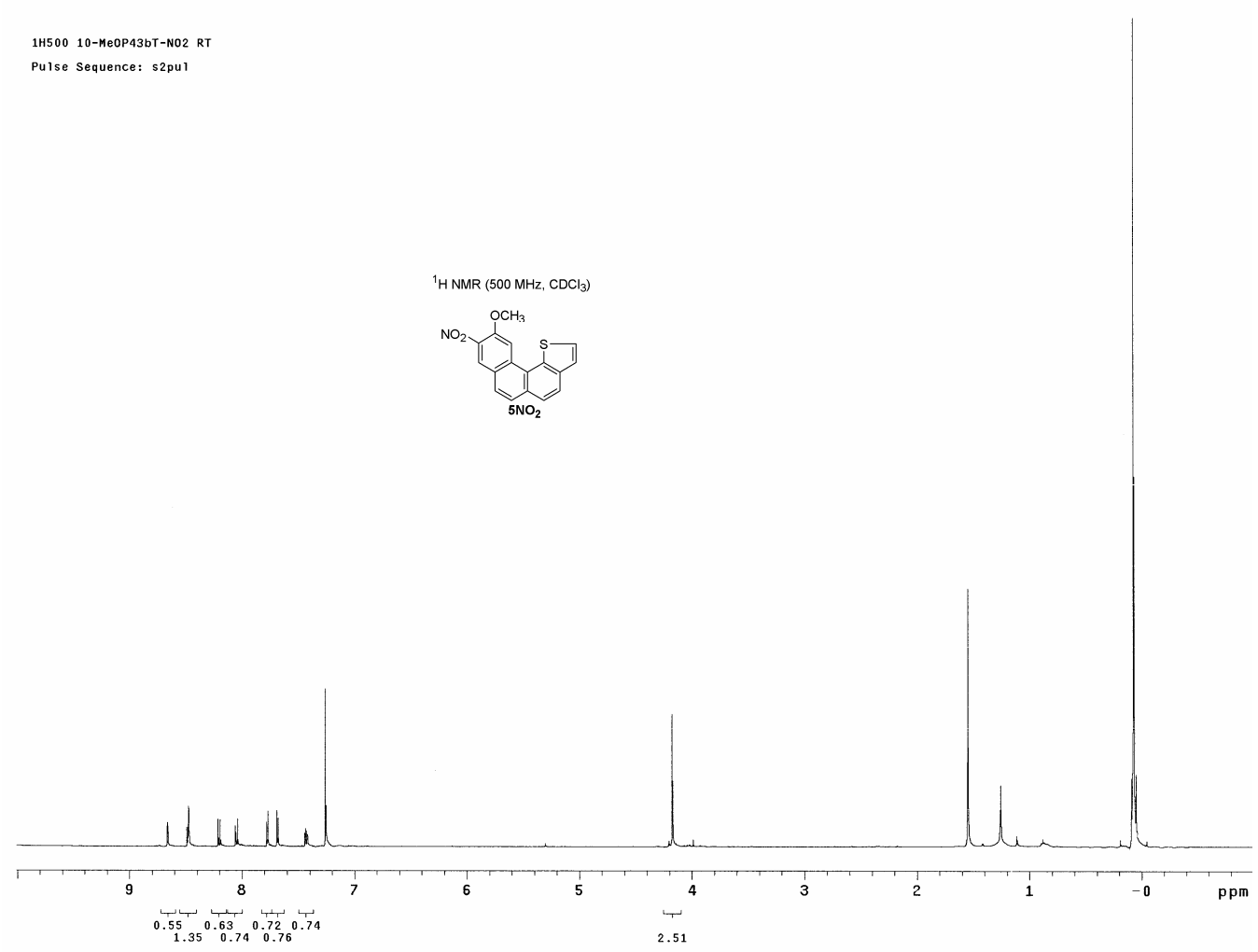

Figure S12. ^{1}H NMR spectrum of **$5NO_2$**.

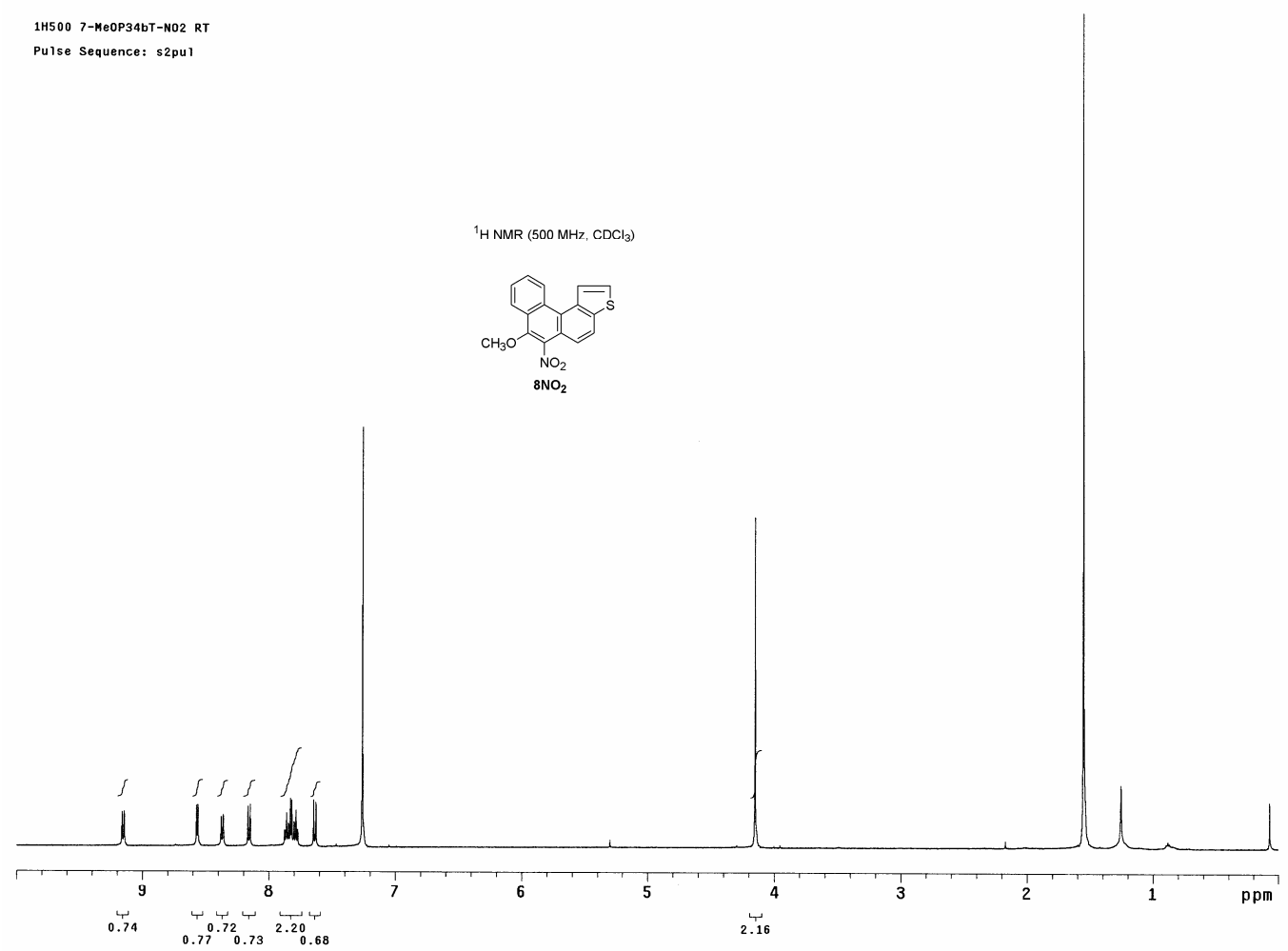

Figure S13. ^{1}H NMR spectrum of **$8NO_2$**.

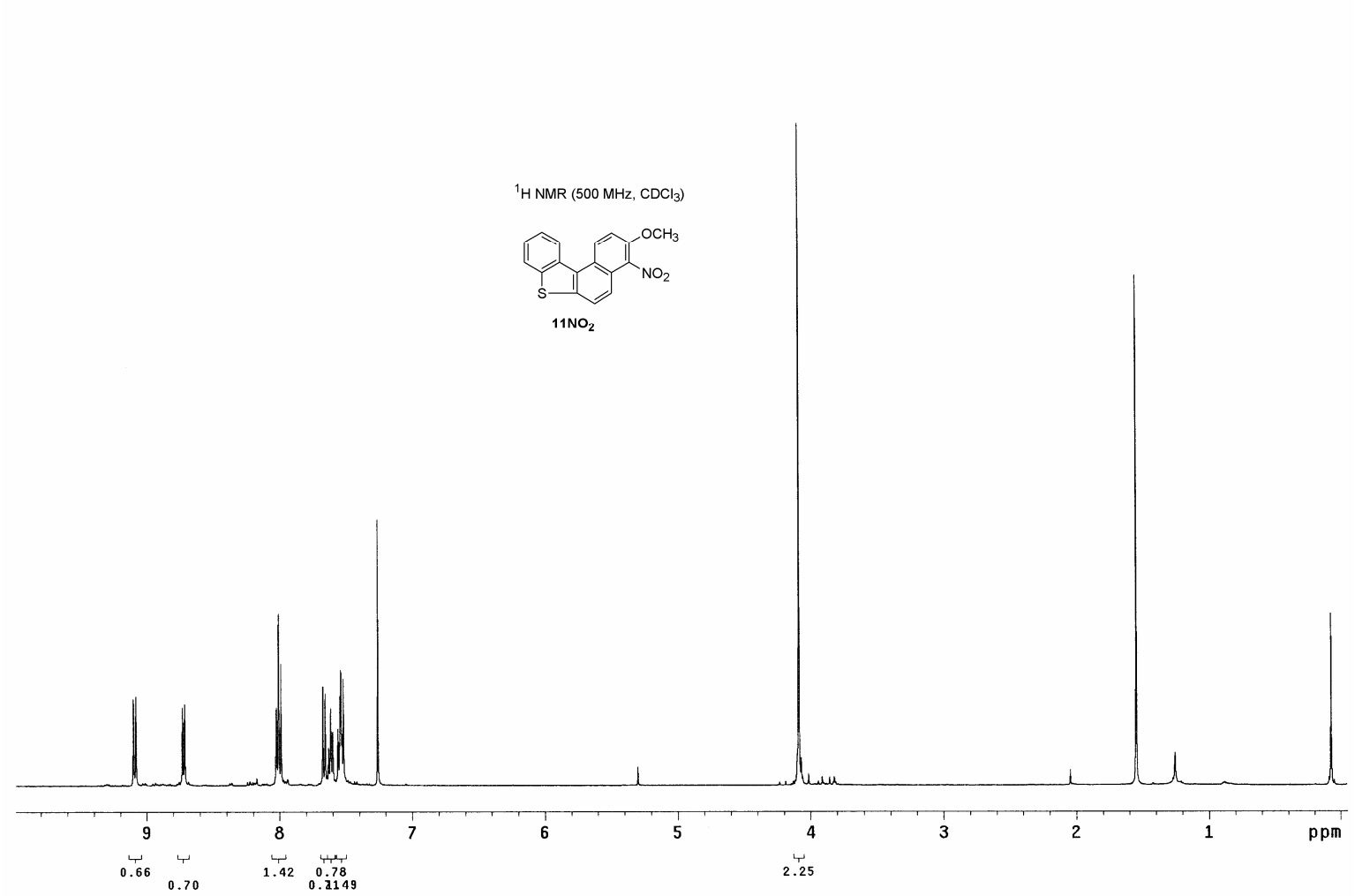

Figure S14. ^{1}H NMR spectrum of **11NO_2**.

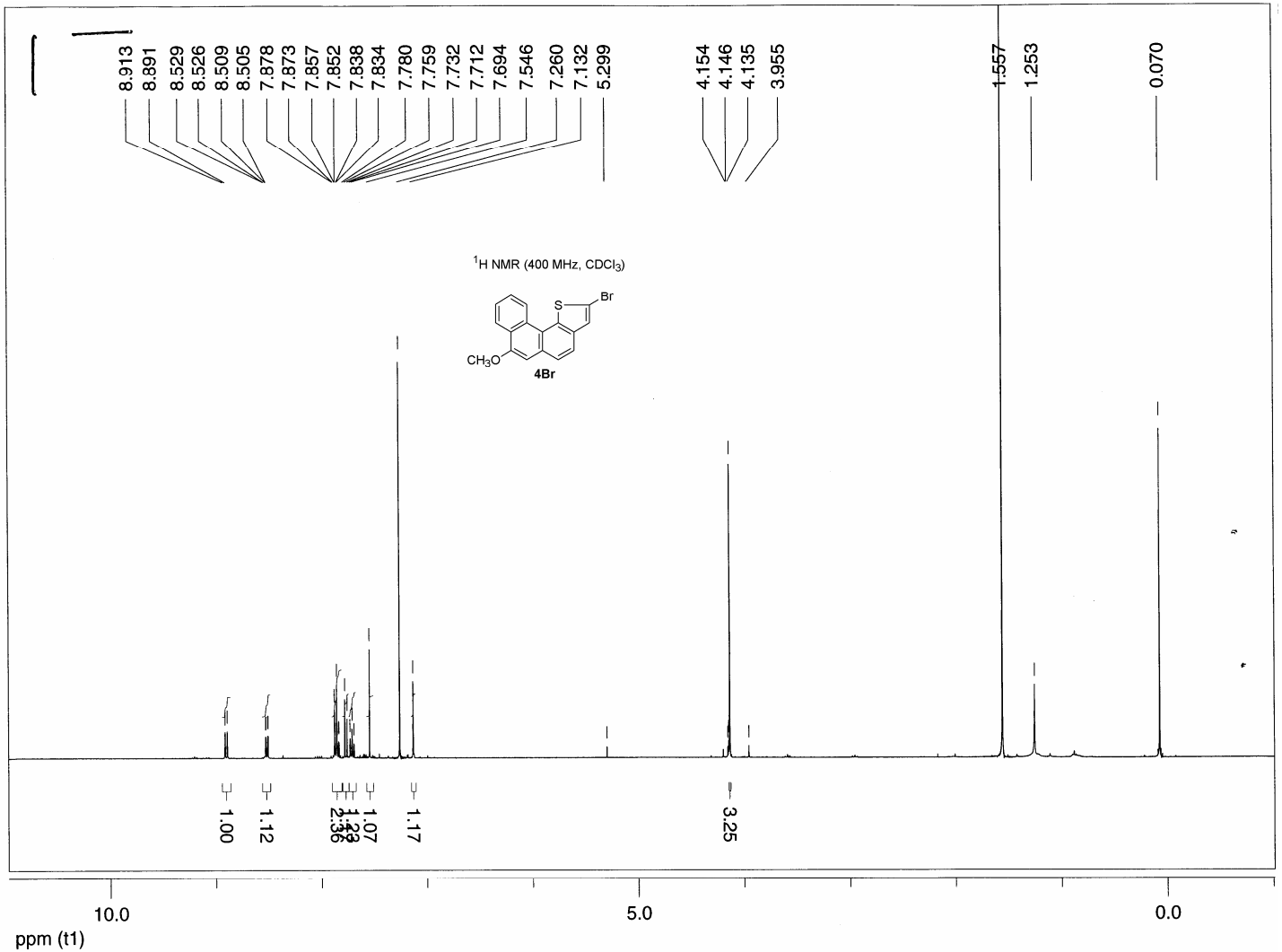

Figure S15. ^{1}H NMR spectrum of **4Br**.

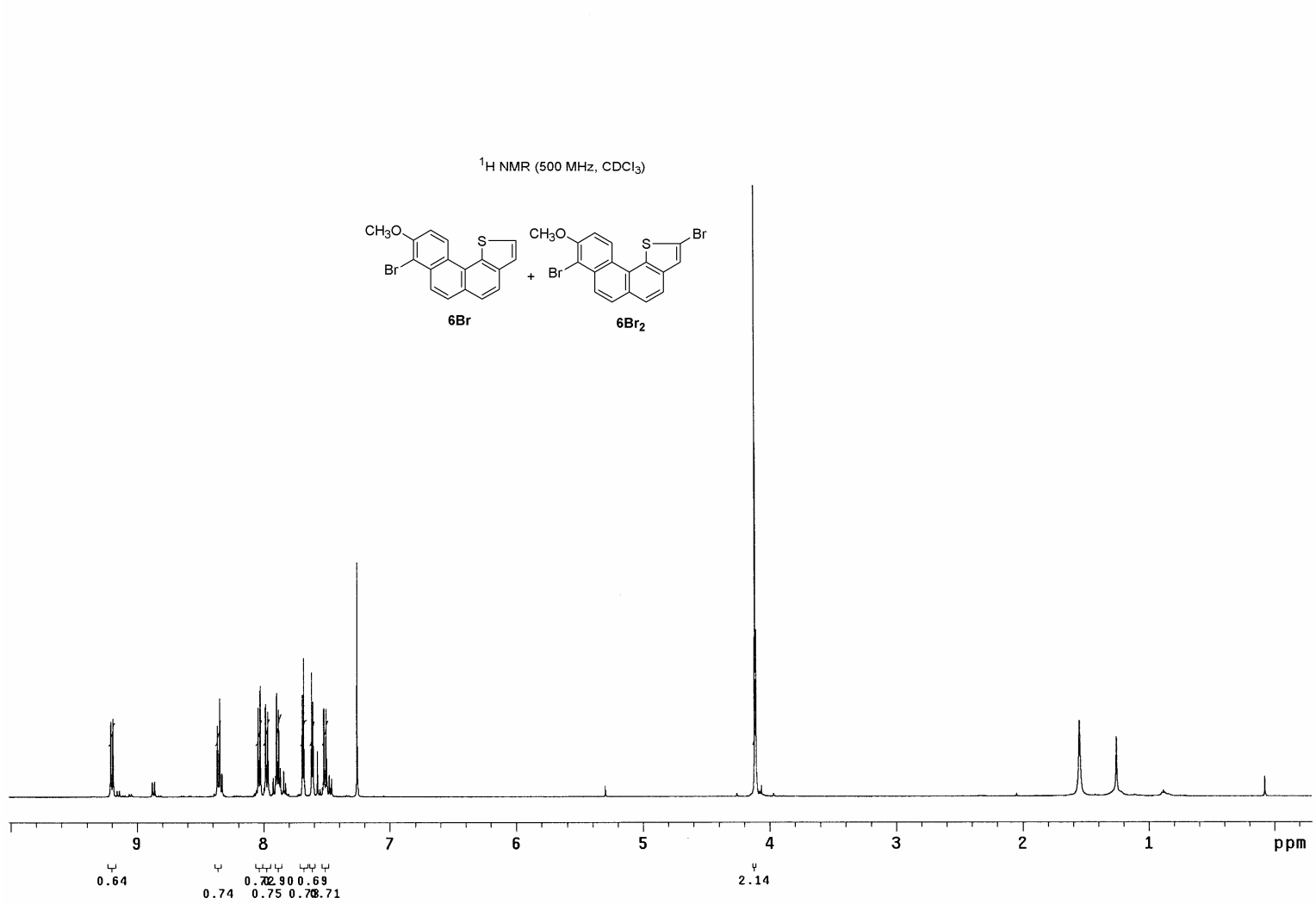

Figure S16. ^{1}H NMR spectrum of isomeric mixture of **6Br** and **$6Br_2$**.